

Chapter 30

Oxygen Isotope Dynamics of Atmospheric Nitrate and Its Precursor Molecules

Greg Michalski, S.K. Bhattacharya, and David F. Mase

Abstract The stable oxygen isotopic composition of atmospheric nitrate is a powerful proxy for assessing what oxidation pathways are important for converting nitrogen oxides into nitrate. Large ^{18}O enrichments and excess ^{17}O (i.e. mass independent composition) are observed in atmospheric nitrate collected across the globe. These isotope enrichments and their variability in space and time have been linked to the magnitude of ozone oxidation. Attempts to model the oxygen isotope enrichments using simplified isotope mass balance assumptions and photochemical models have yielded reasonably good agreement between observations and simulations. However, there is a lack of atmospheric nitrate isotope measurements across a range of different atmospheric environments. Isotopes of oxygen in atmospheric nitrate can be utilized to assess changes in atmospheric chemistry, applied as tracers in nitrate deposition studies, and used to assess the atmosphere's chemical response to environmental change over time using ice core nitrate.

30.1 Introduction

The oxidation of nitrogen compounds into nitrate in the atmosphere is an important mechanism in atmospheric chemistry that controls the transport of this biogeochemically important element. Oxides of nitrogen ($\text{NO}_x = \text{NO} + \text{NO}_2$) are emitted as a by-product

of combustion processes, with anthropogenic emissions from coal burning power plants and automobiles dominating global atmospheric inputs (Galloway et al. 2004; Galloway 1998). However, NO_x is also formed by natural processes such as biogenic nitrification or denitrification (Mosier et al. 1998) and lightning (Martin et al. 2007). A major fraction of NO_x is oxidized in the atmosphere to nitric acid, which is a strong acid that can dramatically lower the pH of precipitation (Rodhe et al. 2002; Galloway 1995). Nitric acid can also react with NH_3 or alkaline dust, generating new aerosols or altering the chemical composition and size of existing particles (Zhang et al. 2000). Atmospheric nitrate ($\text{HNO}_{3(\text{g})}$, $\text{NO}_{3(\text{s})}^-$, $\text{NO}_{3(\text{aq})}^-$) that is removed from the atmosphere by dry and wet deposition is an important new source of N to surface waters, soils, and plant canopies that in turn can impact the function of many ecosystems (Bobbink et al. 2010). Therefore, identifying the mechanisms that transform NO_x into nitrate is key to understanding the natural and human impacted nitrogen cycles from local to regional and global scales.

The use of multiple oxygen isotopes to understand NO_x oxidation in the atmosphere is a recent development. Oxygen has three stable isotopes with approximate mole fractions of: ^{16}O (0.9976), ^{17}O (0.0004) and ^{18}O (0.0020). The international reference material for oxygen is Vienna Standard Mean Ocean Water (V-SMOW) with accepted ratios of 2.0052×10^{-3} for $^{18}\text{O}/^{16}\text{O}$ and 3.827×10^{-4} for $^{17}\text{O}/^{16}\text{O}$ (Kaiser 2009).

The three stable oxygen isotopes normally fractionate in a mass dependant manner, therefore an approximately linear relationship exists between changes in $\delta^{18}\text{O}$ and $\delta^{17}\text{O}$ (Miller 2002). This linearity can be expressed as (Matsuhisa et al. 1978)

G. Michalski (✉) and D.F. Mase
Purdue University, 550 Stadium Mall Drive, West Lafayette,
IN 47907-1210, USA
e-mail: gmichals@purdue.edu; dmase@purdue.edu

S.K. Bhattacharya
Physical Research Laboratory, Navrangpura, Ahmedabad, India
e-mail: bhattacha@prl.res.in

$$\delta^{17}\text{O} = 0.52 \cdot \delta^{18}\text{O} \quad (30.1)$$

A plot of $\delta^{17}\text{O}$ vs. $\delta^{18}\text{O}$ (dual isotope ratio plot) values of the main oxygen reservoirs on Earth, including silicate and carbonate rocks (Miller 2002), waters (Meijer and Li 1998), and oxygen in air (Luz and Barkan 2005) confirms this theoretical relationship, and the resulting line is referred to as the oxygen isotope terrestrial fractionation line (TFL – Fig. 30.1).

One notable exception to this mass dependence rule is the isotopic fractionation that occurs during ozone formation (Thiemens et al. 2001; Thiemens and Heidenreich 1983), when the $^{18}\text{O}/^{16}\text{O}$ and $^{17}\text{O}/^{16}\text{O}$ ratios become equally elevated ($\sim 60\text{--}100\text{‰}$ relative to initial O_2). Since the enrichment is nearly the same in both minor isotopes, independent of their mass difference, this process has been termed a mass independent fractionation (MIF) and is quantified approximately by (Miller 2002).

$$\Delta^{17}\text{O} \sim \delta^{17}\text{O} - 0.52 \cdot \delta^{18}\text{O} \quad (30.2)$$

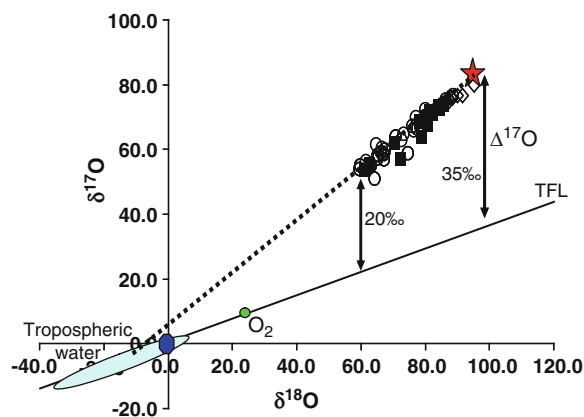


Fig. 30.1 The terrestrial fractionation line (TFL) of oxygen based on the mass dependence of isotope kinetic and equilibrium fractionations that follow $\delta^{17}\text{O} = 0.52 \delta^{18}\text{O}$. The 0.52 coefficient is an average of values that range from 0.5 to 0.53 depending on temperature and the thermodynamics of many reactions (Matsuhisa et al. 1978). The data points show the range of $\Delta^{17}\text{O}$ ($\Delta^{17}\text{O} \sim \delta^{17}\text{O} - 0.52 \cdot \delta^{18}\text{O}$) in atmospheric nitrate from mid-latitudes (Michalski et al. 2003; Kaiser et al. 2007; Morin et al. 2009; Patris et al. 2007). The red star is the approximate triple isotope composition of tropospheric ozone (Johnston and Thiemens 1997; Krankowsky et al. 1995), the blue oval is the range of tropospheric water, and atmospheric O_2 and V-SMOW are the green and blue dots respectively. The atmospheric nitrate data suggest a mixing line between tropospheric ozone and water, in agreement with our mass balance model

Here, MIF has a specific meaning: reactants, whose isotopic compositions lie on the TFL, react and generate products that are offset from the TFL resulting in positive (or negative) $\Delta^{17}\text{O}$ values. In other words, MIF is a chemical process. On the other hand, non-zero $\Delta^{17}\text{O}$ values can be produced either by MIF or by isotope mass balance. For example, when ozone, a powerful oxidizer, transfers O atoms to products during chemical reactions the resulting products have positive $\Delta^{17}\text{O}$ values (Lyons 2001; Michalski and Bhattacharya 2009; Savarino et al. 2000, 2008).

Oxygen isotope compositions in atmospheric nitrate are due to the mixing of oxygen sources (e.g. O_3 , H_2O , O_2) and kinetic and/or equilibrium effects occurring when NO_x is photochemically converted into nitrate. Large $\Delta^{17}\text{O}$ values (23–31‰) observed in atmospheric nitrate (Sect. 30.3) suggest ozone plays an important role as an oxygen source. Tropospheric ozone is also known to have high $\delta^{18}\text{O}$ values ($\sim 80\text{--}130\text{‰}$ V-SMOW) (Sect. 30.5.1) that can be transferred to nitrate and this transfer may partially explain the elevated $\delta^{18}\text{O}$ values observed in atmospheric nitrate (Sect. 30.3). There are other sources of oxygen, however, that are also important during NO_x oxidation, as are the kinetic/equilibrium isotope fractionations that occur during the multiple steps of oxidation. Unfortunately there is currently limited data and little discussion on their importance in controlling the $\delta^{18}\text{O}$ values of atmospheric nitrate. This review will present the current state of knowledge on the chemistry that controls the oxygen isotope composition of atmospheric nitrate, their potential to increase our understanding of NO_x oxidation in the atmosphere, and what future research is needed to maximize this potential.

30.2 Methods for Oxygen Isotope Analysis of Nitrate

The initial analytical approaches for $\delta^{18}\text{O}$ and $\Delta^{17}\text{O}$ analysis of nitrate were pyrolysis techniques. The first reported nitrate pyrolysis technique used a mixture of KNO_3 and $\text{Hg}(\text{CN})_2$ heated to 550°C and isotopic analysis was carried out on the product CO_2 after offline purification (Amberger and Schmidt 1987). Similar offline pyrolysis methods were developed

using a mixture of nitrate salts and graphite, sealed in quartz tubes and heated to 800°C (Revesz et al. 1997; Silva et al. 2000; Wassenaar 1995). This became the preferred method due to the toxicity risks associated with handling cyanide and mercury compounds. Later it was reported that at 800°C the silicate in the quartz reaction vessels would exchange oxygen, to varying degrees, with the product gases. This introduced analytical biases and high uncertainties in data generated using this method (Michalski et al. 2002; Revesz and Böhlke 2002). Kornexl et al. (1999) converted KNO_3 to CO_2 using a high temperature pyrolysis (1,400°C) with a graphite/glassy carbon reaction tube that resolved the exchange problem. In addition, this technique utilized thermal conversion elemental analyzer (TC/EA) devices that could be automated when interfaced with continuous flow isotope ratio mass spectrometer (CF-IRMS) systems. The precision using the TC/EA techniques for nitrate isotopic analysis is ± 0.7 per mil for $\delta^{18}\text{O}$. The first technique for $\Delta^{17}\text{O}$ analysis in nitrate was the thermal decomposition of AgNO_3 (520°C) followed by IRMS analysis of the product O_2 (Michalski et al. 2002). The relatively low decomposition temperature limited the amount of oxygen exchange with the pre-treated quartz reaction tubes and resulted in highly precise $\Delta^{17}\text{O}$ determination ($\pm 0.3\%$). One drawback of the various pyrolysis techniques is the need for rather large amounts of nitrate ($\sim 10^{-5}$ – 10^{-6} mol), which is usually found only in trace amounts in the environment, and makes it difficult to obtain sufficient sample size. In addition, the steps needed to purify environmental samples, such as removing other anions and organic matter, can be inefficient and time consuming (Chang et al. 1999; Michalski 2009).

The size and purification limitations of the pyrolysis methods were largely overcome by the development of the bacterial nitrate reduction technique. The technique is suitable for isotopic analysis of nanomolar amounts of nitrate and requires limited sample preparation. Casciotti et al. (2002) developed the technique, which uses *Pseudomonas aureofaciens* bacteria to produce N_2O that is then analyzed for $\delta^{18}\text{O}$ using CF-IRMS. The key is finding suitable bacteria that lack nitrous oxide reductase activity and do not initiate exchange between nitrogen oxide intermediates and cellular water during the reduction. The reported precision of $\delta^{18}\text{O}$ using the bacteria technique is $\pm 0.5\%$. This technique was modified to analyze $\Delta^{17}\text{O}$ by

Kaiser et al. (2007) who reacted the product N_2O over gold (Cliff and Thiemens 1994) to produce N_2 and O_2 and determined the $\Delta^{17}\text{O}$ on the product O_2 by CF-IRMS with a precision of $\pm 0.6\%$.

A third method for measuring $\delta^{18}\text{O}$ in nitrate is the reduction-azide technique (McIlvin and Altabet 2005). This approach first reduces nitrate to nitrite using spongy cadmium. Nitrite is then converted to N_2O by reaction with hydrazoic acid and isotopic analysis is carried out on the N_2O using headspace extraction and CF-IRMS. During the azide-nitrite reaction, roughly 20% of the oxygen in the product N_2O is derived from water in the reactant solution, requiring a significant correction to the data. The $\delta^{18}\text{O}$ precision using the reduction-azide technique is $\pm 0.5\%$. The azide technique was recently modified to determine $\Delta^{17}\text{O}$ using CF-IRMS by converting the product N_2O into O_2 and N_2 over heated gold (Komatsu et al. 2008) with a precision in $\Delta^{17}\text{O}$ of ± 0.2 , and 0.2% for $\delta^{18}\text{O}$.

All of the above methods require standardization of the analysis using nitrate reference materials in order to attain accurate nitrate $\Delta^{17}\text{O}$ and/or $\delta^{18}\text{O}$ values. This is particularly true for $\Delta^{17}\text{O}$ analysis which is very sensitive to oxygen blanks arising from exchange reactions or air O_2 . The only available $\Delta^{17}\text{O}$ reference material to date is USGS-35, a NaNO_3 from the Atacama Desert, which was developed for nitrate $\Delta^{17}\text{O}$ analysis (Michalski et al. 2002). Additional nitrate reference salts have been developed to span a range of $\delta^{18}\text{O}$ and $\delta^{15}\text{N}$ values as discussed by Böhlke et al. (2003) and are available through the National Institute of Science and Technology (NIST).

30.3 Observations of $\Delta^{17}\text{O}$ and $\delta^{18}\text{O}$ in Atmospheric Nitrate

There are a number of studies on the spatial and seasonal variation of oxygen isotopes in atmospheric nitrate. The first study measuring $\delta^{18}\text{O}$ in precipitation nitrate showed that the atmospheric nitrate $\delta^{18}\text{O}$ values were very elevated relative to V-SMOW ranging from +55 to +72‰ (Durka et al. 1994; Kendall 1998). Subsequent studies extended the range of values from +25 to +115‰ (Fig. 30.2). Notable annual variations were observed, with higher atmospheric nitrate $\delta^{18}\text{O}$ values being found in the colder months and

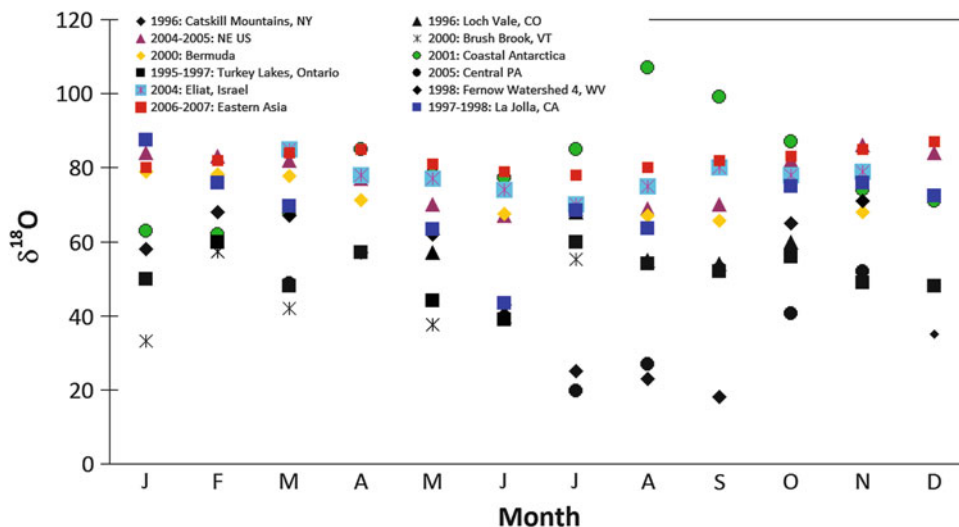


Fig. 30.2 Seasonal variation in $\delta^{18}\text{O}$ values of atmospheric nitrate collected from mid latitude and polar region sites. Individual data sets show that atmospheric nitrate $\delta^{18}\text{O}$ values are usually elevated in the winter months relative to summer. Note data from Savarino et al. data (*green colored circle*) is from Antarctica, where the seasons are out of phase relative to the northern hemisphere. *Black symbols* are data produced using the thermal reduction of nitrate by graphite in quartz tube. *Color*

symbol data was obtained either by the silver nitrate decomposition or bacterial reduction methods. Uncertainty for any given measurement (± 0.4) is the size of the data symbols. Data is from Durka et al. (1994), Morin et al. (2007), Savarino et al. (2006), Spoelstra et al. (2001), Burns and Kendall (2002), Campbell et al. (2002), Hales et al. (2007), Hastings et al. (2003), Michalski et al. (2003), Elliott et al. (2009), Patris et al. (2007), Morin et al. (2009), and Buda and DeWalle (2009)

lower values in the warmer months. Studies conducted at high latitudes (Morin et al. 2007; Savarino et al. 2006; Spoelstra et al. 2001) also show that atmospheric nitrate had elevated $\delta^{18}\text{O}$ values relative to the mid-latitudes. Nitrate $\delta^{18}\text{O}$ values (Fig. 30.2) in precipitation collected in the Catskill Mountains of New York (Burns and Kendall 2002), the Loch Vale watershed, Colorado (Campbell et al. 2002), and Brush Brook, Vermont (Hales et al. 2007), tended to be lower than the $\delta^{18}\text{O}$ values at other mid-latitude sites including Bermuda (Hastings et al. 2003), La Jolla, California, (Michalski et al. 2003), the Northeastern United States (Elliott et al. 2009), coastal sites (Michalski et al. 2003; Patris et al. 2007) and from aerosols over the Atlantic ocean (Morin et al. 2009). The former studies utilized the graphite reduction method (Silva et al. 2000) whereas the latter studies used either the denitrifier (Casciotti et al. 2002) or the AgNO_3 thermal decomposition method (Michalski et al. 2002). It is probable that the studies with lower $\delta^{18}\text{O}$ values suffer from the oxygen exchange analytical bias that leads to a decrease in the nitrate's $\delta^{18}\text{O}$

value (Michalski et al. 2002; Revesz and Böhlke 2002). However, Xue et al. (2010) demonstrated that the graphite- AgNO_3 method produces $\delta^{18}\text{O}$ results that compare well with those obtained using the denitrifier method, suggesting that these low $\delta^{18}\text{O}$ values may be valid.

The first $\Delta^{17}\text{O}$ measurement in atmospheric nitrate was reported by Michalski et al. (2003). This study analyzed aerosols collected over a 1 year period from a coastal urban site in southern California. A seasonal oscillation in the atmospheric nitrate $\Delta^{17}\text{O}$ values was observed, ranging from 23‰ during the summer/spring to 31‰ in the winter months. This was attributed to ozone oxidation chemistry during the conversion of NO_x into HNO_3 (see Sects. 30.5 and 30.6). Subsequent studies of $\Delta^{17}\text{O}$ variation in precipitation and aerosols (Fig. 30.3) from several mid-latitude locations showed similar ranges of values (see Fig. 30.3 and references). There are also seasonal trends in atmospheric nitrate $\Delta^{17}\text{O}$ values. They vary between a low of 22 and a high 44‰, with the higher values occurring during colder months, and the low values

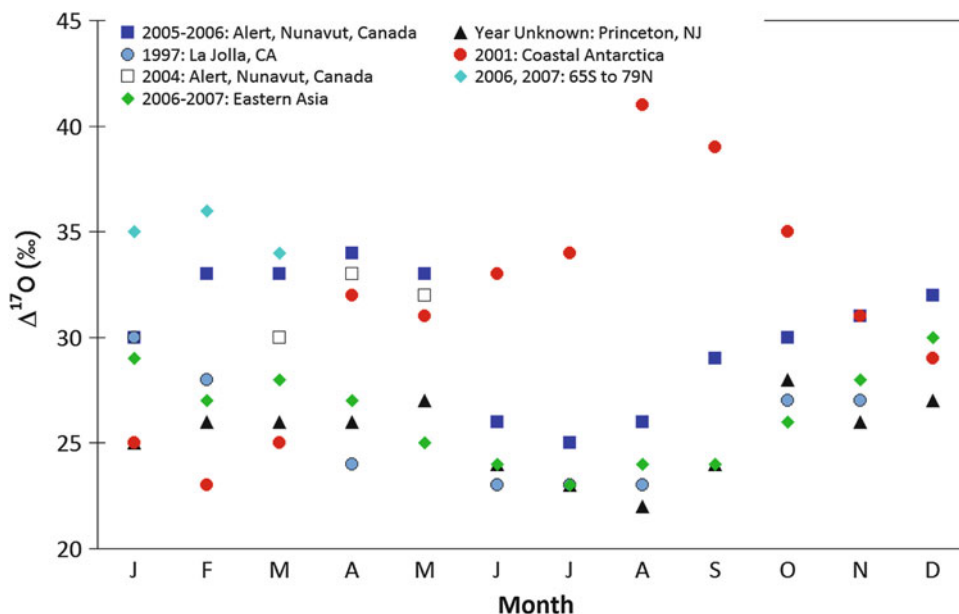


Fig. 30.3 Seasonal trends in the $\Delta^{17}\text{O}$ values of atmospheric nitrate. Nitrate collected in the southern hemisphere (McCabe et al. 2007; Savarino et al. 2007) have the opposite phase relative to northern hemisphere nitrate. Mid-latitude locations have atmospheric nitrate $\Delta^{17}\text{O}$ values that span 20–30‰

(Michalski et al. 2003; Morin et al. 2007; Kaiser et al. 2007; Patris et al. 2007), while polar regions tend to have higher $\delta^{18}\text{O}$ values and more pronounced seasonal trends. Uncertainty for any given $\Delta^{17}\text{O}$ measurement (± 0.4) is the size of the data symbols

occurring during warmer periods, similar to the $\delta^{18}\text{O}$ seasonal trends (Fig. 30.3). Atmospheric nitrate $\Delta^{17}\text{O}$ values also vary with latitude: Summit, Greenland (Kunasek et al. 2008), Alert, Canada (Morin et al. 2008), Dumont d’Urville, Antarctica (Savarino et al. 2006), Northern Ellesmere Island, Canada (Morin et al. 2007), and the South Pole (McCabe et al. 2007) all tend to have higher $\Delta^{17}\text{O}$ values relative to the mid-latitude sites (Michalski et al. 2003; Kaiser et al. 2007; Morin et al. 2009; Patris et al. 2007). The preponderance of studies in polar regions is due to an abundance of interest in using isotopes in ice core nitrate as a proxy for past chemistry/climate change (see Chap. 39 and 40).

The seasonal and spatial trends in atmospheric nitrate $\Delta^{17}\text{O}$ and $\delta^{18}\text{O}$ values are intriguing and suggest that there may be some utility in understanding the underlying mechanisms that cause these trends. The oxidation of NO_x into nitrate is tightly controlled by reactions with ozone (Sect. 30.4), which is also known to have high $\Delta^{17}\text{O}$ and $\delta^{18}\text{O}$ values

(Krankowsky et al. 1995; Johnston and Thiemens 1997). Theoretical models have tried to explain the atmospheric nitrate isotope trends in terms of isotope mass balance mixing models (Michalski et al. 2003; Morin et al. 2007; Alexander et al. 2009; see Sect. 30.6), where different oxidation pathways utilized unique oxygen sources, including ozone. These models suggested that oxygen isotopes in atmospheric nitrate might be used to trace the relative importance of different oxidation pathways (gas phase vs. aerosol reactions) under changing environmental conditions (e.g. polluted, volcanic events, climate change). In addition, since atmospheric nitrate can be incorporated into polar ice caps, nitrate oxygen isotopes might be a new proxy for studying the past oxidation state of the atmosphere (paleo-atmospheric chemistry; see Chap. 39). The theory behind these isotope mass balance models and their ability to reproduce observed isotopic trends in atmospheric nitrate are discussed in the remaining sections of this review.

30.4 Mass Balance Approach to Oxygen Isotope Variation in Atmospheric Nitrate

30.4.1 Isotope Mass Balance During Nitrate Production

When a compound is formed, its isotopic composition is determined by the isotopic composition of the reactants and kinetic or equilibrium fractionation effects that occur during the formation process. For oxygen isotopes, this can be formulated as

$$\delta^{18}\text{O}_{\text{prod}} = \sum a_i \delta^{18}\text{O}_{\text{react } i} + \sum \varepsilon_{\text{rxn } i} \quad (30.3)$$

$$\delta^{17}\text{O}_{\text{prod}} = \sum a_i \delta^{17}\text{O}_{\text{react } i} + \sum \varepsilon_{\text{rxn } i} \quad (30.4)$$

where $\varepsilon_{\text{rxn } i}$ is the temperature dependent kinetic isotope effect (KIE) or equilibrium enrichment factor (in ‰) for the reaction (i), and a_i is the mole fraction of oxygen in the product attained from a given reactant (i). The sums arise when more than one reactant contributes oxygen to the system ($\sum a_i = 1$) and multiple kinetic steps exist in the reaction mechanism. When using an isotope mass balance model, for simplification, the $\varepsilon_{\text{rxn } i}$ of the reactions are ignored. This simplification is used in modeling atmospheric nitrate production because few of the oxygen $\varepsilon_{\text{rxn } i}$ relevant to nitrate production have been measured. This is a limitation, but as experimental or theoretical determinations of these KIE and equilibrium enrichment factors become available they can be incorporated into, and improve, the models.

A similar isotope composition equation can be derived for $\Delta^{17}\text{O}$ values

$$\Delta^{17}\text{O}_{\text{prod}} = \sum a_i \Delta^{17}\text{O}_{\text{react } i} + \sum \Delta \varepsilon_{\text{rxn } i} \quad (30.5)$$

There are relatively few reactions that generate $\Delta^{17}\text{O}$ values in products from reactants that have isotopic compositions on the TFL (Fig. 30.1) i.e. MIF. The MIF enrichment factor for a given reaction (i) is noted as $\Delta \varepsilon_{\text{rxn } i}$ in (30.5). Indeed, ozone formation is the only known tropospheric reaction that has a major MIF (Sect. 30.5.1). This leads to the approximation that, other than ozone production, the $\sum \Delta \varepsilon_{\text{rxn } i} = 0$ for

other atmospheric nitrate production processes and this approximation has been used in models that predict the evolution of $\Delta^{17}\text{O}$ signatures in atmospheric nitrate (Sect. 30.6).

30.4.2 Isotope Mass Balance During Nitrate Removal

Processes that remove a compound through transport or reactivity can also change the isotopic composition of the residual compound. For oxygen isotopes this can be formulated as

$$\delta^{18}\text{O}_{\text{residual}} = \delta^{18}\text{O}_{\text{initial}} - \sum \varepsilon_{\text{rxn } i} \quad (30.6)$$

$$\Delta^{17}\text{O}_{\text{residual}} = \Delta^{17}\text{O}_{\text{initial}} - \sum \Delta \varepsilon_{\text{rxn } i} \quad (30.7)$$

where $\varepsilon_{\text{rxn } i}$ is the temperature dependent, kinetic or equilibrium fractionation factor of a loss process (i). The loss processes change the isotopic composition of the initial reservoir in a mass dependent manner and they often exhibit Rayleigh distillation-type behavior, where the isotope ratios in the residual reactant change exponentially as a function of the fraction (f) of the compound remaining, which is usually a function of time.

$$\delta^{18}\text{O}_{\text{residual}} = \delta^{18}\text{O}_{\text{initial}} - \varepsilon_{\text{rxn}} \ln[f(t)] \quad (30.8)$$

$$\Delta^{17}\text{O}_{\text{residual}} = \Delta^{17}\text{O}_{\text{initial}} - \Delta \varepsilon_{\text{rxn}} \ln[f(t)] \quad (30.9)$$

The main loss process for atmospheric nitrate is removal by wet and dry deposition. To the best of our knowledge there is no data that has measured the ε_{rxn} for either depositional process, which is a serious limitation when interpreting $\delta^{18}\text{O}$ variations observed in atmospheric nitrate. The $\Delta \varepsilon_{\text{rxn}}$ of wet and dry deposition, however, should follow mass dependent isotope fractionation rules, so $\Delta \varepsilon_{\text{rxn}} \sim 0$ can be assumed. This assumption dictates that nitrate $\Delta^{17}\text{O}$ values are not impacted by the loss process itself. However, in time-dependent models, the loss process can influence the $\Delta^{17}\text{O}$ values of nitrate depending on environmental conditions. This is because evaluating $\Delta^{17}\text{O}$ values in nitrate during each time step requires incorporating the nitrate $\Delta^{17}\text{O}$ values from the previous time step. In

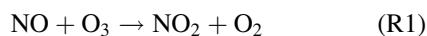
other words, the $\Delta^{17}\text{O}_{\text{residual}}$ term in the loss equation (30.9) must be carried over into the isotope mass balance in the production equation (30.5) at the next time step:

$$\Delta^{17}\text{O}_{(\text{total})} = x(\Delta^{17}\text{O}_{\text{prod}})_t + (1-x)(\Delta^{17}\text{O})_i \quad (30.10)$$

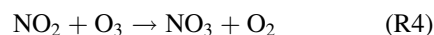
where x is the mole fraction of nitrate produced in the current time step (t) relative to the total amount of nitrate in the atmosphere. In cases where the loss processes are ignored, nitrate builds up in the atmosphere and the instantaneous $\Delta^{17}\text{O}$ value produced in the current time step ($\Delta^{17}\text{O}_{\text{prod}})_t$ becomes less important as x becomes smaller. Such a situation might arise during dry periods in areas below temperature inversions where both deposition mechanisms are minimized. Conversely, if removal is rapid then the nitrate $\Delta^{17}\text{O}$ values will more closely reflect the current chemistry because x is large. This situation might occur during periods of regular precipitation that would scrub nitrate from the atmosphere. The loss processes must also be considered in one, two or three dimensional models. In these models, nitrate produced in an adjacent grid cell with different chemistry and isotopic ratios can be transported into the grid cell under consideration, changing the isotopic composition of the nitrate depending on nitrate production/transport ratio.

30.4.3 Oxygen Isotope Mass Balance During Nitrate Production

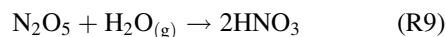
Nitrate production is initiated by the oxidation of NO. The first step is the conversion of NO into NO_2 , which can occur by oxidation by either ozone (R1) or peroxy radicals (R3). The majority of peroxy radicals are produced when radical species such as H, CH_3 , and R (where R is an organic radical), combine with atmospheric O_2 (R2).



Therefore, in order to use the isotope mass balance simplification in the NO oxidation step, the $\delta^{18}\text{O}$ and $\Delta^{17}\text{O}$ values of tropospheric O_3 and O_2 need to be known, which is discussed in Sects. 30.5.1 and 30.5.4, respectively. More oxidized forms of nitrogen, NO_3 and N_2O_5 , are produced by NO_2 oxidation via ozone (R4 and R5). Again, the isotopic mass balance approximation can be used by assuming no KIE during the oxidation and having measured or modeled the isotopic composition of tropospheric ozone (Sect. 30.5.1)



In the final steps of nitric acid formation, two other oxygen sources enter into the equation, OH radicals and liquid water. The primary oxidation pathway for the production of nitric acid is the third body (M) mediated OH oxidation of NO_2 (R6). An important alternative pathway that forms nitric acid is the heterogeneous hydrolysis of N_2O_5 on wet aerosol surfaces (R8). Finally, a minor but non-trivial pathway to nitric acid is through hydrogen abstraction by nitrate radicals (R7). Again, to use an isotope mass balance approach for predicting isotope variation in nitric acid, one needs to know how $\delta^{18}\text{O}$ and $\Delta^{17}\text{O}$ values in tropospheric water (Sect. 30.5.2) and OH radicals (Sect. 30.5.3) vary in space and time.

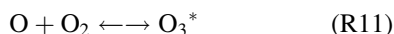
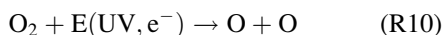


To summarize, in order to predict the isotope composition of atmospheric nitrate using a simple isotope mass balance model, the isotopic composition of tropospheric O_3 , H_2O , OH, and O_2 need to be known (measured) or approximated (modeled).

30.5 Isotopic Composition of Oxygen Sources that Contribute to Nitrate

30.5.1 Oxygen Isotope Composition of Tropospheric O₃

There is a tremendous amount of published research on isotope effects that occur during the formation of ozone (Thiemens et al. 2001; Mauersberger et al. 2003). Ozone formation is initiated when oxygen atoms are produced either by high energy (E) photons/electrons (R10) or through NO₂ photodissociation (see R16 below). O₂ molecules react with ground state oxygen atoms to form an excited ozone complex (R11) that can either decompose or be stabilized to ground state O₃ (R12) by a third body (M):



The isotopic composition of the product ozone is characterized by a large enrichment in the heavy isotopes ¹⁷O and ¹⁸O (relative to ¹⁶O), when compared to the O₂ reactant (Thiemens and Heidenreich 1983; Mauersberger et al. 2001). As mentioned before, not only are the heavy isotopes more abundant, but there is a large MIF (Thiemens and Heidenreich 1983).

Many theoretical attempts have been made to understand the basic principle behind the large MIF associated with ozone formation (Heidenreich and Thiemens 1983; Valentini 1987; Gellene 1996; Gao and Marcus 2001). The most successful is the theory of Hathorn, Gao and Marcus, which uses a modified version of the Rice–Ramsperger–Kassel–Marcus (RRKM) theory of unimolecular decomposition to treat reaction R11 (Gao and Marcus 2001; Hathorn and Marcus 1999; Hathorn and Marcus 2000). Ozone formation is visualized to be a time-dependent competition between unimolecular decomposition (R11) and the collisional stabilization of O₃* (R12). If energy can be shared among the vibrational-rotational modes of the O₃* complex, its lifetime is extended and therefore more O₃ is formed. It has been suggested that the asymmetric ozone isotopomers, with heavy isotopes

at the terminal position, dissociate (R11) slower than symmetric isotopomers due to a larger number of symmetry-allowed mode couplings. Therefore asymmetric ozone, regardless which minor isotope breaks the symmetry, have higher formation rates relative to symmetric species (i.e. ¹⁶O¹⁶O¹⁶O). This leads to the equal enrichment of ¹⁷O and ¹⁸O in the product ozone.

This theoretical model implies that the MIF is driven by a symmetry effect. This would suggest that the non-zero Δ¹⁷O resides only in the molecules of type OOQ (asymmetric) and not in type OQO (symmetric), where Q is either ¹⁷O or ¹⁸O. Any enrichment observed in the symmetrical molecules (like OQO) should follow the mass dependent fractionation relationship. Three experiments have been conducted to test this hypothesis by studying chemical systems where ozone reacts through its terminal position atom: ozone reacting on solid silver foil (Bhattacharya et al. 2008), with NO_(g) (Savarino et al. 2008), and nitrite in solution (Michalski and Bhattacharya 2009). If the bulk ozone Δ¹⁷O anomaly resides only in the terminal position then by mass balance:

$$\Delta^{17}\text{O}(\text{terminal}) = 1.5 \cdot \Delta^{17}\text{O}(\text{bulk}) \quad (30.11)$$

as the central atom would only dilute the anomaly. The isotopic composition of the oxygen atom transferred during these reactions would therefore have Δ¹⁷O 1.5 times the initial ozone if this hypothesis is true. In all three experiments the expected factor of 1.5 is observed (Fig. 30.4) within the uncertainty of the experiments. There are some small discrepancies that need additional investigation, but in general the hypothesis of the anomalous ¹⁷O enrichment residing in the terminal atoms appears to be valid. This is important in the nitrate mass balance models because NO oxidation by O₃ via its terminal atom (R1) would be different if the anomaly were evenly distributed across all oxygen atoms in ozone.

The isotope effects generated during ozone formation have been investigated under a number of conditions. Experiments using either electrical discharge or UV radiation generate product ozone with δ¹⁸O and Δ¹⁷O values in the range of 70–120‰ and 32–45‰ respectively (relative to the initial O₂). This variation is the result of different pressure and temperature conditions under which the ozone is formed. Experiments examining the pressure dependency (Guenther

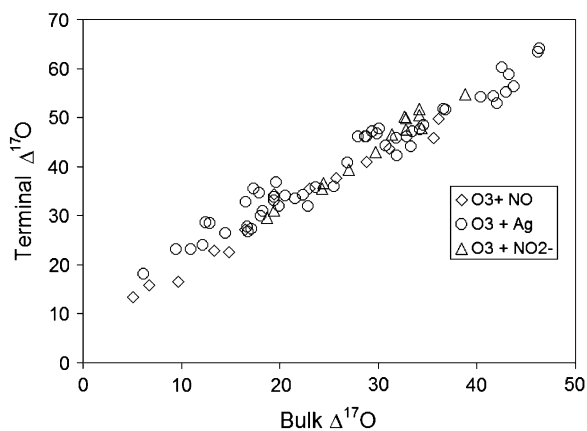


Fig. 30.4 Experiments that assess the terminal atom enrichment in ozone. If the symmetry hypothesis is correct then the terminal atoms should be enriched by a factor of 1.5 relative to the bulk. The terminal enrichment coefficients are 1.63 ± 0.33 (Bhattacharya et al. 2008), 1.59 ± 0.39 (Savarino et al. 2008), and 1.49 ± 0.06 (Michalski and Bhattacharya 2009)

et al. 2000; Thiemens and Jackson 1990) showed that both the $\delta^{18}\text{O}$ and the $\Delta^{17}\text{O}$ enrichments in ozone decrease with increasing pressure (Fig. 30.5) and disappear at very high pressures (Thiemens and Jackson 1990). The experimental pressure dependence of ozone's $\delta^{18}\text{O}$ and $\Delta^{17}\text{O}$ values (at 321 K) can be fitted to an equation in P (pressure in the range 50–800 torr). For pressures typical of the troposphere (500–800 torr), a regression of data reported in Morton et al. (1990) yields the pressure-dependency equation ($\delta^{18}\text{O}_{(\text{ozone})}$ relative to the initial O_2):

$$\delta^{18}\text{O}_{(\text{ozone})} = -0.03P_{\text{torr}} + 112.4 \quad (30.12)$$

The ozone $\delta^{18}\text{O}$ temperature dependency (at 50 torr), can also be found by regressing Morton et al.'s data:

$$\delta^{18}\text{O}_{(\text{ozone})} = 0.52T(\text{K}) - 45 \quad (30.13)$$

Calculating the expected $\delta^{18}\text{O}$ value for ozone in the troposphere, which has variable temperature and pressure, requires corrections based on these equations. Since the reference temperature for the pressure experiments in Morton et al. was 321 K (far higher than the average surface temperature), (30.12) is modified for the temperature difference using $0.52 \cdot (T(\text{K}) - 321)$. In addition, the enrichments determined by

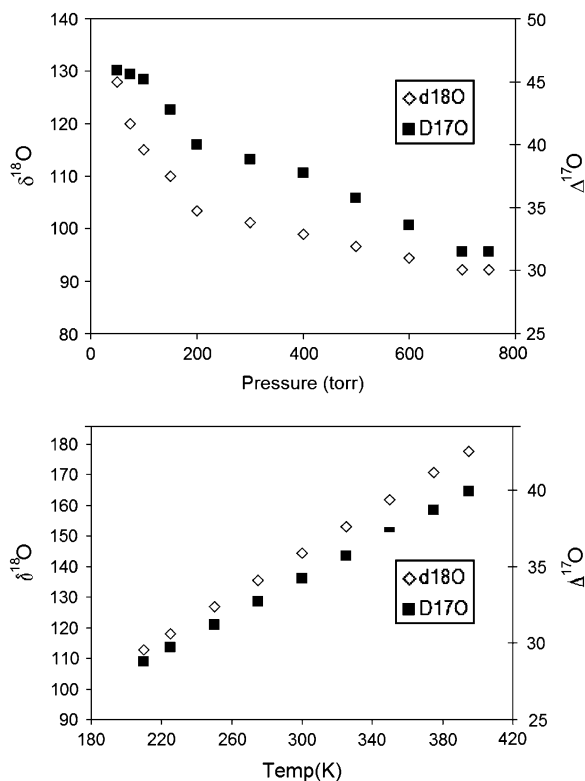


Fig. 30.5 Temperature and pressure dependence of $\Delta^{17}\text{O}$ (solid square) and $\delta^{18}\text{O}$ (open diamond) values generated during ozone production. Data was reproduced by averaging data from Guenther et al. (2000), Thiemens and Jackson (1990), and Morton et al. (1990)

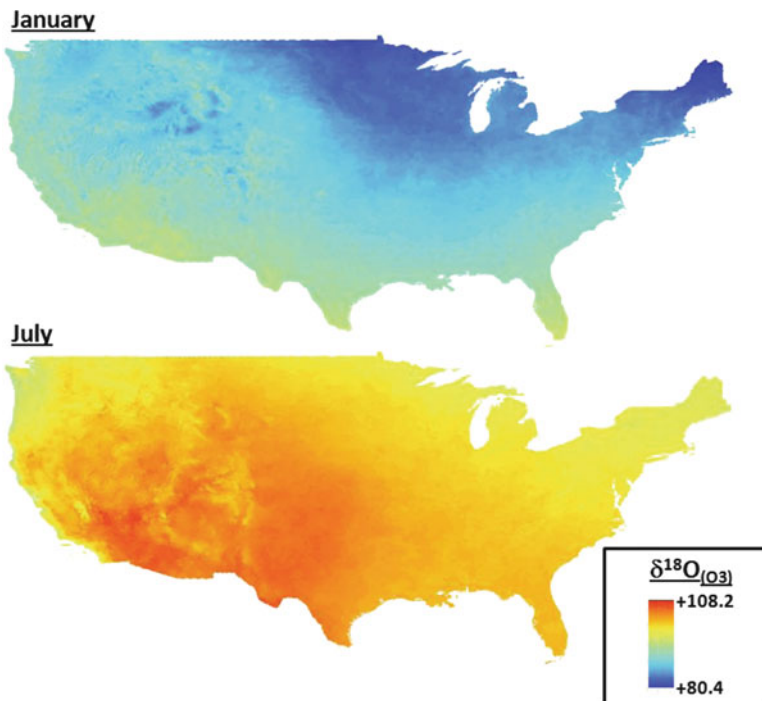
Morton et al. were relative to the initial O_2 composition. In the atmosphere where air O_2 is +23.4‰ relative to V-SMOW (Barkan and Luz 2003), an additional standard correction factor ($\delta_{\text{O}_3\text{-vsmow}} = \delta_{\text{O}_3\text{-air}} + \delta_{\text{air-vsmow}} + \delta\delta^1/1,000$) is applied to the fitted data when using V-SMOW as the reference point yielding:

$$\delta^{18}\text{O}_{(\text{ozone})} = (-0.028P_{\text{torr}} + 134.8) + [0.52 \cdot (T(\text{k}) - 321)] \quad (30.14)$$

Using (30.14) and pressure/temperature estimates from the North American Regional Reanalysis (NARR) dataset (Kalnay et al. 1996), we calculated the spatial variability of the predicted $\delta^{18}\text{O}$ values of ozone over the continental US (Fig. 30.6). The predicted $\delta^{18}\text{O}$ values (80–108‰) span the same range as those observed in tropospheric ozone collected in southern California (95–115‰V-SMOW) by Johnston

Fig. 30.6 Spatial and seasonal variation of ozone $\delta^{18}\text{O}$ variation across the continental US for January 1 and July 1 of 2001.

The values are calculated using (30.14) and the NARR temperature and pressure data. The predicted range of ozone $\delta^{18}\text{O}$ values is $\sim 28\%$ and tracks with temperature in regions with minimal topography and pressure in mountainous regions



and Thiemens (1997). However, the observed ozone $\delta^{18}\text{O}$ values are always higher ($\sim 3 - 18\%$) relative to those predicted by our P/T model when using temperature and pressures at the California site during collection times. The other tropospheric ozone $\delta^{18}\text{O}$ dataset collected in Germany (Krankowsky et al. 1995) has ozone values spanning $100 - 130\%$, again higher than our model predictions. One factor for this discrepancy is that the average surface temperature and pressure are used to calculate the $\delta^{18}\text{O}$ values in Fig. 30.6, when average boundary layer temperatures and pressures may be more appropriate. Another possibility for the discrepancy is KIE associated with O_3 dry deposition or photolysis reactions that may leave the residual O_3 enriched (Liang et al 2006). The ozone $\delta^{18}\text{O}$ observations were limited in their spatial and temporal scope, therefore it is difficult to evaluate whether extrapolating the laboratory based data to atmospheric conditions is rigorously reflecting ozone $\delta^{18}\text{O}$ value or if the ozone $\delta^{18}\text{O}$ measurements are inaccurate, but in general there is relatively good agreement between model estimated and observed tropospheric ozone $\delta^{18}\text{O}$ values.

Temperature (Morton et al. 1990) and pressure data (Thiemens and Jackson 1990; Guenther et al. 2000)

was also fitted to assess how $\Delta^{17}\text{O}$ values might vary in the atmosphere. Fitting these data sets yields pressure (P at constant 321 K) and temperature (T at constant 50 torr) $\Delta^{17}\text{O}$ equations

$$\Delta^{17}\text{O} = 78.8P^{-0.122} \quad (30.15)$$

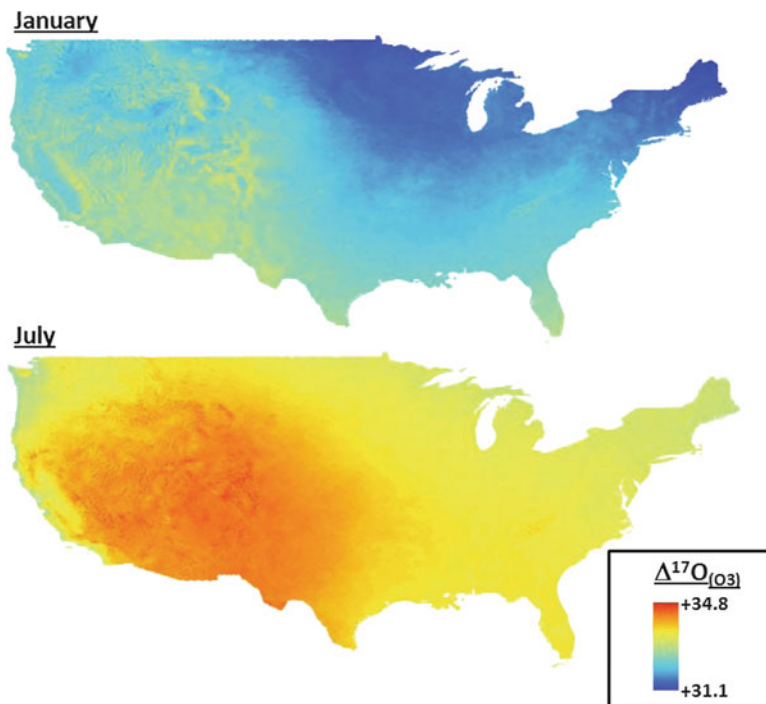
$$\Delta^{17}\text{O} = 16.2 + 0.06 \cdot T(\text{K}) \quad (30.16)$$

Normalizing to the experimental temperature (i.e. as in (30.14)) gives

$$\Delta^{17}\text{O} = (78.8P^{-0.122}) + 0.06 \cdot (T(\text{K}) - 321) \quad (30.17)$$

Using NARR temperature and pressure data and (30.17) we have estimated the winter and summer ozone $\Delta^{17}\text{O}$ values over the continental US (Fig. 30.7). The predicted ozone $\Delta^{17}\text{O}$ values span a relatively narrow range, from 31 to 35‰, and they generally follow the seasonal change in temperature, but low pressure at high altitudes is also a factor (Fig. 30.7). These predicted values are close to observed $\Delta^{17}\text{O}$ values of ozone collected at the White Mountain Research Station (27–35.8‰) but higher

Fig. 30.7 Modeled ozone $\Delta^{17}\text{O}$ values across the US for January 1 and July 1, 2001. Total variation is less than 5‰ and mainly correlates with temperature, with lower ozone $\Delta^{17}\text{O}$ values in flat regions and cooler climates, where surface pressure varies by only tens of millibars. However, pressure is clearly a factor in mountainous regions in the western US, where the $\Delta^{17}\text{O}$ increases with decreasing pressure. The data is generated using (30.17) and the mean daily temperature and pressure from the NARR dataset



than $\Delta^{17}\text{O}$ values of tropospheric ozone sampled from coastal (20–35.8‰; average 26.4‰, $n = 29$) and urban (19–22‰; average 21.2‰, $n = 7$) sites in Southern California (Johnston and Thiemens 1997). The discrepancy between the modeled $\Delta^{17}\text{O}$ values (Fig. 30.7) and the observations is likely due to the difficulties encountered using the ozone collection system, which may lead to isotopic fractionation, exchange, or contamination. Resolving this discrepancy between predicted $\delta^{18}\text{O}$ and $\Delta^{17}\text{O}$ values of tropospheric ozone at a given pressure and temperature is an area of active research.

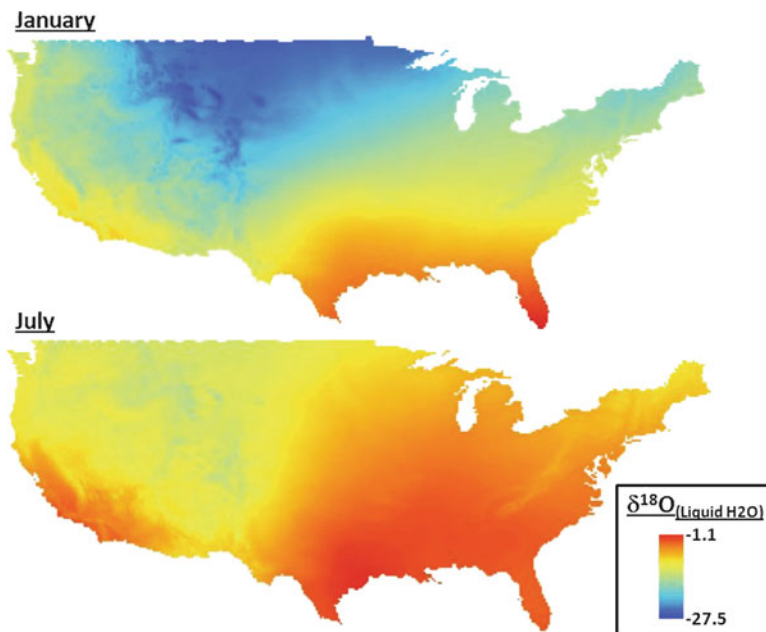
30.5.2 Oxygen Isotopic Composition of Tropospheric Water

There is a tremendous amount of data on the isotopic composition of water in the troposphere, stemming largely from the efforts of the Global Network of Isotopes in Precipitation (GNIP) (IAEA/WMO 2006). GNIP and other organizations at various local levels have compiled $\delta^{18}\text{O}$ and δD values in precipitation across many sites over the past 40 years (Araguas-Araguas et al.

2000; Vuille et al. 2005). The GNIP data and spatial interpolation techniques have been used to model continuous global spatial variations of water $\delta^{18}\text{O}$ values (Bowen and Revenaugh 2003). The interpolated data is available in a number of formats but the Water-isotopes.org web site (<http://wateriso.eas.purdue.edu/waterisotopes/>) is a very user-friendly resource. Complete details of water isotope variations and their use are detailed in Chap. 33).

Water does not act as an oxidant during the conversion of NO_x into nitrate, but it does act as an oxygen source during several steps in the oxidation scheme. Therefore, understanding its variation is important for understanding the variability of $\Delta^{17}\text{O}$ and $\delta^{18}\text{O}$ in nitrate. Water in the troposphere has a $\Delta^{17}\text{O}$ value of approximately 0 (Meijer and Li 1998), though small variations of up to 0.08‰ have been detected using high precision techniques (Barkan and Luz 2005; Uemura et al. 2010). Conversely, tropospheric water $\delta^{18}\text{O}$ values are highly variable and are a function of the source of the water (i.e. oceanic, lake, evapotranspiration) and the temperature of evaporation and condensation (Gat 1996). The lowest precipitation $\delta^{18}\text{O}$ values are found at the poles (−70‰) and highs (+10‰) are usually found in arid environments.

Fig. 30.8 Estimated $\delta^{18}\text{O}$ values for precipitation water across the contiguous United States for January and July of 2001, based on interpolation (from <http://www.waterisotopes.org>)



Spatial trends in water isotopes are often addressed in terms of latitudinal effects, longitudinal effects and altitude effects (Gat 1996). The interpolated model of variations in the $\delta^{18}\text{O}$ of precipitation across the continental US for January and June of 2001 is shown in Fig. 30.8.

Water can be incorporated into nitrate during NO_x oxidation from both the liquid and gas phase. Liquid water is incorporated into nitrate when N_2O_5 is converted to HNO_3 on wetted aerosol surfaces (R8). Since N_2O_5 is nitric acid anhydride, this occurs fairly rapidly (Hallquist et al. 2000; Mentel et al. 1999), although there are still some uncertainties concerning what role aerosol composition plays in the efficiency of N_2O_5 uptake (Brown et al. 2003). Current models (Alexander et al. 2009; Michalski et al. 2003) assume that there is no additional exchange between aerosol water and N_2O_5 during the hydrolysis but this has yet to be shown experimentally. Once formed, the exchange between water and nitrate is negligible except under extremely low pH conditions (Böhlke et al. 2003; Bunton et al. 1952). The gas phase reaction between $\text{H}_2\text{O}_{(\text{g})}$ and N_2O_5 (R9) is believed to be too slow to be a significant source of HNO_3 (Tuazon et al. 1983; Wahner et al. 1998).

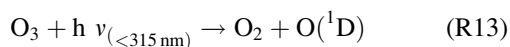
Water in the gas phase can also be incorporated into nitrate via the NO_2 reaction with OH (R6). OH can

exchange with gas phase water (Dubey et al. 1997) and the $\delta^{18}\text{O}$ of OH will ultimately be dependent on the $\delta^{18}\text{O}$ of water vapor with which it exchanges. Temperature dependent variations in water vapor enrichment factors, relative to the liquid water, can be fitted by inverting the experimental data for the temperature dependent $\text{H}_2\text{O}_{(\text{g})} \leftrightarrow \text{H}_2\text{O}_{(\text{l})}$ equilibrium (Horita and Wesolowski 1994; Majoube 1971)

$$\begin{aligned} \varepsilon_{\text{g-l}} = 1,000 \ln \alpha_{(\text{g})} = & -7.685 + 6.7123(1,000/T) \\ & - 1.6664(10^6/T^2) + 0.35041(10^9/T^3) \end{aligned} \quad (30.18)$$

30.5.3 Oxygen Isotope Composition of Tropospheric OH

The OH radical is the dominant oxidizer in the atmosphere and is a key oxidizer of NO_2 because of the gas phase reaction that leads to nitric acid (R6) with a rate constant of $2.8 \times 10^{-11} \text{ cm}^3 \text{ molecule}^{-1} \text{ s}^{-1}$ (at 300 K, 101 kPa). OH is formed by the production of $\text{O}(^1\text{D})$ atoms via ozone photolysis that react with water vapor



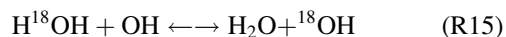
Because of OH's high reactivity and low steady state concentration (10^5 – 10^6 molecules cm^{-3}) there are, however, no direct measurements of its isotopic composition in the troposphere. By isotope mass conservation (R13 and R14) the isotopic composition of OH should be a mixture of ozone and tropospheric water vapor. However, the OH radical is capable of exchanging with water vapor (R15) with a Arrhenius rate constant of $2.3 \times 10^{-13} \exp[(2,100(\pm 250))/T] \text{ cm}^3 \text{ molecule}^{-1} \text{ s}^{-1}$ (Dubey et al. 1997). At 300 K this is a relatively slow reaction ($3 \times 10^{-16} \text{ cm}^3 \text{ molecule}^{-1} \text{ s}^{-1}$). However, if the ratio (ρ) of the rate of exchange relative to the rate of reaction with NO_2 (R6) is high (>10) the exchange would dominate and equilibrium be essentially achieved:

$$\rho = k_{\text{R15}}[\text{H}_2\text{O}]/k_{\text{R6}}[\text{NO}_2] \quad (30.19)$$

Under most NO_x scenarios ($\text{NO}_2 < 1$ ppbv) and water mixing ratios (~ 0.01), ρ is on the order of 10^1 – 10^3 . However, under high NO_x (10 ppbv) and/or low water mixing ratios (5×10^{-3} and $\sim 50\%$ relative humidity at 275 K) the isotope exchange can become comparable to reactivity rates. But these cases are rare (Morin et al. 2008); so under most circumstances it can be approximated that OH achieves equilibrium with water vapor. This exchange would eliminate any $\Delta^{17}\text{O}$ transfer during reaction R14. This is not true for the stratosphere or polar regions, where water is at ppmv levels, and OH may retain its ozone $\Delta^{17}\text{O}$ signature (Lyons 2001).

Because of this exchange reaction, the $\delta^{18}\text{O}$ values of OH in the troposphere will be a function of the $\delta^{18}\text{O}$

of the water vapor in the air mass and the fractionation factor for the equilibrium reaction



Using observed water isotopologue vibrational frequencies (Herzberg 1966), the OH vibrational frequency (Dieke and Crosswhite 2010), and the reduced mass, simple harmonic oscillator approximation, the reduced partition functions of OH and water isotopologues can be determined as a function of temperature (Urey 1947). Calculating the isotope enrichment factor over a tropospheric temperature range of 250–310 K and fitting the data yields a temperature dependent fractionation factor for OH given by:

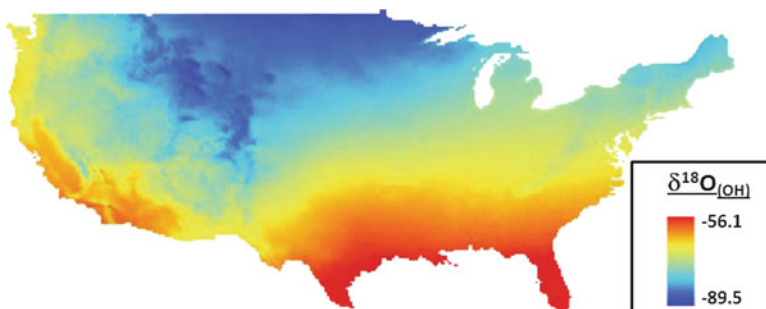
$$\varepsilon = 1,000 \ln \alpha = 0.188T - 99.3 \quad (30.20)$$

This equation predicts that OH should be depleted by roughly 44‰ relative to atmospheric water vapor at 298 K. Using the $\delta^{18}\text{O}$ of tropospheric water (Fig. 30.8) and (30.18) and (30.20), the $\delta^{18}\text{O}$ of OH over the continental US was modeled (Fig. 30.9). This estimate of the $\delta^{18}\text{O}$ of OH does not consider any of the KIE arising during the reactions between OH and the numerous organic compounds in the atmosphere and should only be taken as a first order approximation.

30.5.4 Oxygen Isotope Composition of Tropospheric O_2

Atmospheric O_2 is incorporated into nitrate via the oxidation of NO by peroxy radicals (R3) formed from O_2 reactions with H and organic radicals (R2).

Fig. 30.9 Modeled $\delta^{18}\text{O}$ values of OH for January 1, 2001. The values are determined using modeled water vapor $\delta^{18}\text{O}$ assuming equilibrium with liquid water (30.18) and the calculated OH-water equilibrium fractionation factor (30.20)

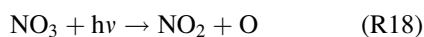
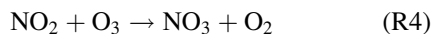
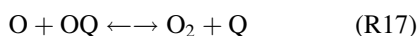
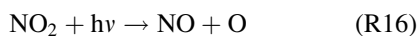
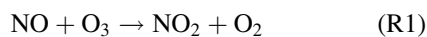


The $\delta^{18}\text{O}$ value of atmospheric oxygen is $\sim 23\%$ relative to V-SMOW, a value that is controlled by the balance between photosynthesis and respiration isotope effects, known as the Dole effect (Dole et al. 1954). Because of its huge abundance and the well-mixed nature of the troposphere, there is essentially no spatial or temporal variation in tropospheric O_2 $\delta^{18}\text{O}$ values. Measurement of the $\delta^{17}\text{O}$ value of atmospheric O_2 relative to V-SMOW indicates a small negative $\Delta^{17}\text{O}$ value for O_2 (Luz et al. 2005; Barkan and Luz 2003). This negative anomaly can be explained by isotopic mass balance when stratospheric oxygen atoms derived from ozone impart MIF to CO_2 (Thiemens et al 1991; Yung et al. 1991).

30.6 Modeling Oxygen Isotope Variation in Atmospheric Nitrate

30.6.1 Oxygen Isotope Variation in NO_x

Atmospheric nitrate is derived from NO_x and its oxygen isotope composition is dependent on isotope effects associated with the NO_x cycle. The NO_x cycle is initiated by NO oxidation by ozone, which is then followed by photolysis of NO_2 by solar actinic flux and the subsequent reformation of O_3



During this cycling, isotope exchange between oxygen atoms and O_2 is rapid (R17) and this equilibration erases any isotope effect that might have carried over from NO_2 formation or photolysis. During the O_3 formation process, however, large $\delta^{18}\text{O}$ and

$\Delta^{17}\text{O}$ values are generated during the recombination reaction (Sect. 30.5.1). The transfer of heavy isotopes from ozone to NO_2 during R1 leads to a NO_x - O_3 equilibrium as a quasi steady state balance of these reactions develops. This has recently been demonstrated experimentally (Michalski et al. in preparation).

The dynamics of the NO - O_3 reaction system and the internal distribution of isotopes in ozone are important controls on the isotopic composition of the product NO_2 . As discussed in Sect. 30.5.1 the isotope anomaly ($\Delta^{17}\text{O}$) and some of the ^{18}O enrichment is found in the terminal atom of O_3 , via the so-called symmetry effect. If NO reacts with ozone through a terminal atom transition state, as shown by ab initio calculations (Peiro-Garcia and Nebot-Gil 2002), then the heavy isotope transfer will be larger than if all three oxygen atoms in ozone reacted with equal probability. Savarino et al. (2008) evaluated the fractionation between ozone and NO_2 during NO oxidation, a combination of the internal distribution of ^{18}O in ozone and the KIE of the reaction itself. The experiments conducted at pressures and temperatures typical of the troposphere showed a $\delta^{18}\text{O}$ correction factor of 0.83 (Savarino et al. 2008). We applied this correction factor to (30.14), which yields a T-P equation that predicts the $\delta^{18}\text{O}$ value (V-SMOW) of the oxygen atom transferred to NO_2 during NO oxidation:

$$\delta^{18}\text{O}_{(\text{trans})} = 0.83 * \{(-0.028P_{\text{torr}} + 134.8) + [0.52 * (T(\text{k}) - 321)]\} \quad (30.21)$$

The same experiment examined the $\Delta^{17}\text{O}$ transfer during the oxidation via R1 and showed that the branching ratio of the reaction for the central atom in ozone is only 0.08 suggesting that the terminal abstraction pathway is dominant (Savarino et al. 2008). Using this branching ratio and the terminal only enrichment hypothesis (30.11) yields a $\Delta^{17}\text{O}$ value of the oxygen atom transferred from ozone to NO_2 during NO oxidation as:

$$\Delta^{17}\text{O}_{\text{O}_{\text{NO}+\text{O}_3}} = 1.5 * 0.92 * \Delta^{17}\text{O}_{\text{O}_3(\text{bulk})} \quad (30.22)$$

Using the modeled $\Delta^{17}\text{O}_{\text{O}_3(\text{bulk})}$ for the continental US (Fig. 30.7) would yield a typical NO_x - O_3 equilibrium value of $\sim 46\%$. A more realistic experiment recently examined the isotope effect during the full

NO_x equilibrium (Michalski et al. in preparation), and generated $\Delta^{17}\text{O}$ value in NO_2 of $\sim 45\text{‰}$, in excellent agreement with Savarino et al. (2008).

30.6.2 Box Model Evaluation of $\Delta^{17}\text{O}$ Variations in Atmospheric Nitrate

Several zero dimensional photochemical box models have been used to simulate $\Delta^{17}\text{O}$ variations in atmospheric nitrate (Michalski et al. 2003; Morin et al. 2008; Michalski and Xu 2010). The models calculate how much atmospheric nitrate is produced by reactions R6, R7, and R8. In each of these pathways the main reactant is NO_2 , or higher oxides of nitrogen derived from NO_2 ; therefore, the first step is to assess NO_2 $\Delta^{17}\text{O}$ either directly (see Sect. 30.6.1) or calculate it based on the $\Delta^{17}\text{O}$ of ozone and the reaction dynamics. However, under natural conditions peroxy radical (ROO) oxidation of NO (R3) is an alternative mechanism for generating NO_2 . This pathway can be significant depending on local concentrations of organic compounds and NO_x (Jaegle et al. 2000). In the case of ROO, the oxygen atom transferred to NO_2 is derived from reactions of organic radicals with O_2 (R2) which has a $\Delta^{17}\text{O} \sim 0\text{‰}$ (Sect. 30.5.4). Therefore, one can define an oxidation parameter, ϕ , which is the mole fraction of NO oxidation by ozone relative to total NO oxidation: $\phi = \text{R1}/(\text{R1} + \Sigma\text{R3's})$. The term ΣR3 arises because a number of organo-peroxy and HO_x radicals are capable of oxidizing NO to NO_2 . Based on this, the $\Delta^{17}\text{O}$ of NO_2 ($\Delta^{17}\text{O}_{\text{NO}_2}$) in the troposphere is estimated to be

$$\Delta^{17}\text{O}_{\text{NO}_2(\text{trop})} = \phi \Delta^{17}\text{O}_{\text{NO}_2(\text{exp})} = \phi \Delta^{17}\text{O}_{\text{O}_3\text{trans}} \quad (30.23)$$

where $\Delta^{17}\text{O}_{\text{NO}_2(\text{exp})}$ is the experimental $\Delta^{17}\text{O}$ of NO_2 in the NO_x - O_3 equilibrium experiment (Michalski et al. in preparation) or the $\Delta^{17}\text{O}$ value of the terminal oxygen atom (P,T dependent) that equilibrates with NO_x (Savarino et al. 2008).

Based on the inspection of reactions R6, R7, and R8 and using the approximation that H_2O , O_2 , and OH all have $\Delta^{17}\text{O}$ values of $\sim 0\text{‰}$ (see Sect. 30.5), a set of $\Delta^{17}\text{O}$ mass balance equations can be derived (Michalski et al. 2003):

$$\Delta^{17}\text{O}_{\text{HNO}_3(\gamma)} = \Delta^{17}\text{O}_{\text{O}_3} \cdot (2\phi/3), \quad (30.24)$$

$$\Delta^{17}\text{O}_{\text{HNO}_3(\eta)} = \Delta^{17}\text{O}_{\text{O}_3} \cdot (2\phi + 1)/3, \quad (30.25)$$

$$\Delta^{17}\text{O}_{\text{HNO}_3(\phi)} = \Delta^{17}\text{O}_{\text{O}_3} \cdot (4\phi + 1)/6, \quad (30.26)$$

where ϕ is the mole fraction of NO oxidized by O_3 , and γ , η , and ϕ are the mole fractions of HNO_3 produced by the reaction pathways R6, R7, and R8 respectively. Predicting $\Delta^{17}\text{O}$ anomalies in atmospheric nitrate ($\Delta^{17}\text{O}_{\text{HNO}_3}$) is then a matter of estimating the $\Delta^{17}\text{O}$ value of O_3 (or NO_2) and calculating the mole fractions (ϕ, γ, η, ϕ) using a photochemical kinetics model. $\Delta^{17}\text{O}$ values are calculated in each time step and normalized to the total nitrate produced during the simulation.

Several box model systems have been used to simulate atmospheric nitrate $\Delta^{17}\text{O}$ data. The first study (Michalski et al 2003) utilized a box model for simulating nitrate production in a polluted marine boundary layer (Yvon et al. 1996). There was reasonably good agreement between the observed $\Delta^{17}\text{O}$ values of atmospheric nitrate and the predicted values, but during the spring there were predicted-observed differences of up to 5‰. This was attributed to the model's inability to account for transport of atmospheric nitrate from neighboring regions by advective flow. Morin et al. (2008) estimated atmospheric nitrate $\Delta^{17}\text{O}$ values by adapting CiTTyCAT (Cambridge Transport Trajectory model of Chemistry And Transport), a photochemical box model previously used to examine the origin of polluted layer in the North Atlantic (Wild et al. 1996). This model's predictions agreed reasonably well with observed $\Delta^{17}\text{O}$ variations in the Arctic (Morin et al. 2008). Michalski and Xu (2010) used the regional atmospheric chemical mechanism (RACM) (Stockwell et al. 1997) and the $\Delta^{17}\text{O}$ mass balance approximation (ISO-RACM = isotope RACM) to assess changes in $\Delta^{17}\text{O}$ over a wide range of atmospheric parameters (Fig. 30.10). Using the terminal atom $\text{O}_3 + \text{NO}$ reaction mechanism, ISO-RACM predicts a range $\Delta^{17}\text{O}$ values that is similar to that observed in the atmosphere (Figs. 30.3 and 30.10). The simulations also tested the sensitivity of atmospheric nitrate $\Delta^{17}\text{O}$ predictions to a range of atmospheric parameters including temperature, relative humidity, trace gas concentrations, and surface solar radiation (actinic flux). Atmospheric nitrate $\Delta^{17}\text{O}$

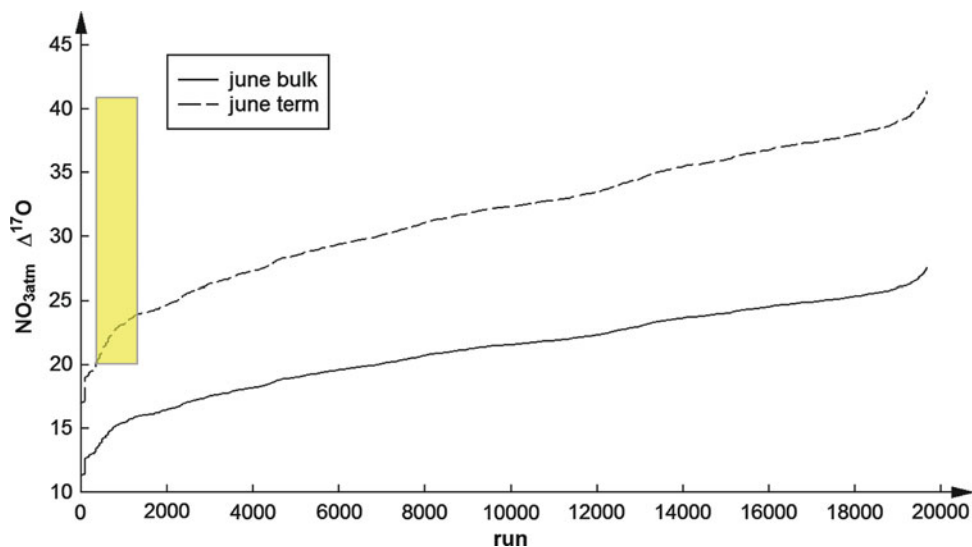


Fig. 30.10 Simulated $\Delta^{17}\text{O}$ values of atmospheric nitrate under a wide range of simulated atmospheric conditions (NO_x , organic compounds, temperature, humidity, etc.) for June (each run is a different set of conditions). Recent experiments have

provided new evidence that the “bulk transfer” mechanism is not likely to be valid but rather it is the terminal mechanism (Savarino et al. 2008). All observed data (yellow box) fall within the predicted range when using the terminal mechanism

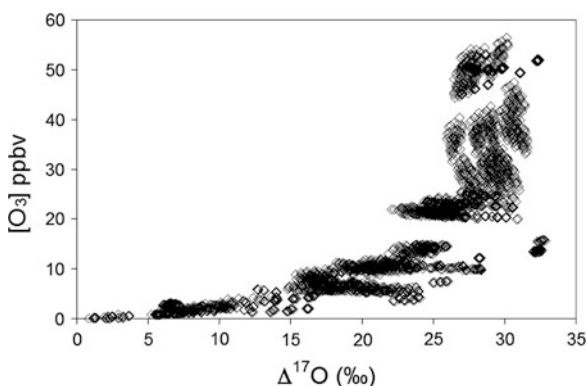


Fig. 30.11 Variation of atmospheric nitrate $\Delta^{17}\text{O}$ values as a function of O_3 mixing ratios. The graph highlights that by observing atmospheric nitrate, inferences can be made about the oxidation state of the atmosphere (i.e. importance of ozone or peroxy radicals). This highlights the potential for using atmospheric nitrate contained in ice cores as a proxy for changes in oxidative potential

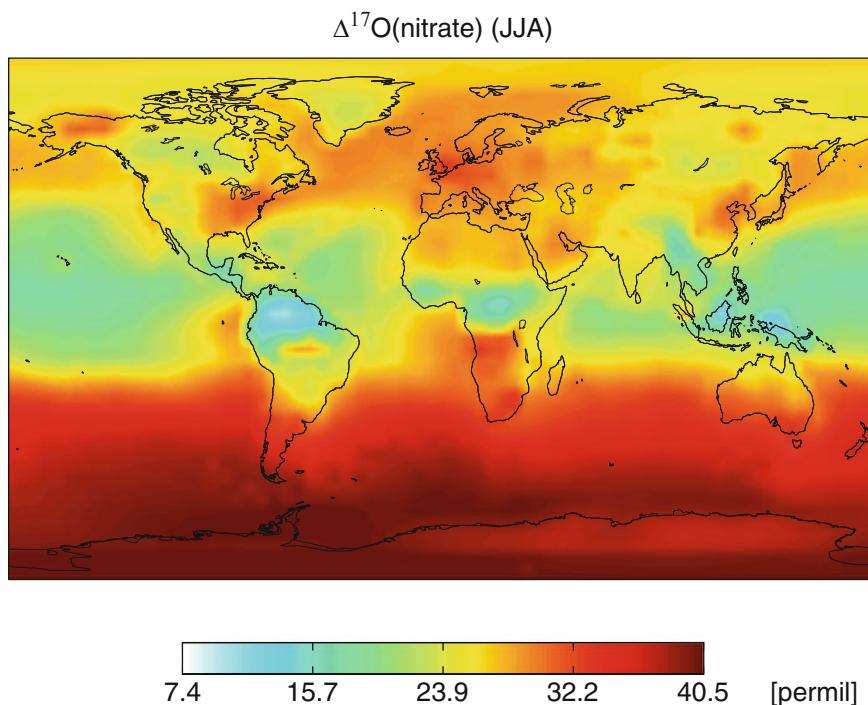
values were found to be sensitive to actinic flux, with increased fluxes (longer days during spring/summer) generating lower $\Delta^{17}\text{O}$ values in agreement with observed seasonal trends (Fig. 30.3). This effect is derived from smaller ϕ values with increased sunlight through increased production of peroxy radicals and higher γ values driven by the increase of NO_2 oxidation by OH during sunlight conditions. Atmospheric

nitrate $\Delta^{17}\text{O}$ values were also sensitive to concentration of certain trace gases. While variations in methane and carbon monoxide mixing ratios had little influence on predicted $\Delta^{17}\text{O}$ values, the trace gases such as NO_x , volatile organic compounds, and ozone clearly influenced the predicted $\Delta^{17}\text{O}$ values by shifting nitrate production pathways. For example, higher $\Delta^{17}\text{O}$ values were predicted at higher O_3 mixing ratios relative to low levels (Fig. 30.11).

30.6.3 3D Modeling of Nitrate $\Delta^{17}\text{O}$ Values

Global variations in atmospheric nitrate $\Delta^{17}\text{O}$ values were recently modeled using a 3D chemical transport model GEOS-Chem (Alexander et al. 2009). The model uses the same simple mass balance approach discussed above. The GEOS-Chem model does have the advantage of being able to include vertical and horizontal transport, and incorporates spatial variations in surface fluxes of important primary pollutants such as NO_x and VOC's, which is a serious limitation in the box models. Full details of the model resolution, fluxes, chemistry, etc. can be found in Alexander et al. (2009).

Fig. 30.12 Predicted global $\Delta^{17}\text{O}$ values in atmospheric nitrate for boreal summer using GEOS-Chem 3D chemical transport model (Alexander et al. 2009). Clear latitudinal $\Delta^{17}\text{O}$ variations are simulated and are the result of a combination of daylight hours, peroxy radical oxidation, and shifts in the relative importance of nitrate production pathways R6–R8. Such spatial heterogeneity of atmospheric nitrate $\Delta^{17}\text{O}$ values have not been verified by measurements



The GEOS-Chem model predicts atmospheric nitrate $\Delta^{17}\text{O}$ values that generally fall within the range of observations (Fig. 30.12). Globally, $\Delta^{17}\text{O}$ values range from a low of $\sim 7\text{‰}$ up to a maximum of 41‰ and exhibit a similar seasonal variation (high in winter, low in summer) as observations (Sect. 30.3). The model tends to over predict $\Delta^{17}\text{O}$ values in the mid to high latitudes in winter and underestimates them in polar regions during the spring and summer. The model attributes the seasonal $\Delta^{17}\text{O}$ variation in atmospheric nitrate to changes in the relative amount of NO oxidized by O_3 (ϕ) and seasonal changes in the relative importance of the N_2O_5 hydrolysis (φ). This study also supports the hypothesis that change in the oxygen isotopes in atmospheric nitrate reflects changes in oxidation chemistry in the atmosphere.

The purpose of both the box model and 3D simulations is to try and rationalize the atmospheric nitrate $\Delta^{17}\text{O}$ measurements in the context of changes in atmospheric chemistry. Shifts to peroxy radical (R3) and OH (R6) oxidation will lead to lower $\Delta^{17}\text{O}$ values. This will tend to happen in regions with high volatile organic carbon emissions and abundant sunlight (Alexander et al. 2009; Michalski and Xu 2010) such as the tropics. Conversely, N_2O_5 (R8) and O_3 (R1)

oxidation push atmospheric nitrate $\Delta^{17}\text{O}$ values higher. The N_2O_5 reaction is a strong function of aerosol surface area, aerosol type, limited sunlight and temperature (at cold temperature the R5 equilibrium favors N_2O_5). This reaction would be favored in the high latitude during winter when it is cold and dark. Therefore, the objective is to use the isotopes to understand the chemistry and how that might change under anthropogenic and natural environmental perturbations.

Two things are required for the predictions of atmospheric nitrate $\Delta^{17}\text{O}$ models to converge with observations (1) A detailed understanding of the isotope effects arising during different steps of NO_x oxidation (2) Confidence in the chemical and biogeochemical mechanisms in the model itself (i.e. reaction rates, uptake coefficients, emission inventories, meteorology etc.). This review has focused on the former rather than the latter. This is because the model mechanisms have been extensively dealt with by the larger atmospheric chemistry community. Conversely, research on the isotopic effects in the NO_x – NO_y system has only recently been developed and the largest error in the predictions is likely to come from the unknowns in these effects. If these uncertainties in the

isotope mechanisms can be significantly reduced, then atmospheric nitrate $\Delta^{17}\text{O}$ values may be a new way of validating the chemical models themselves.

30.6.4 Modeling $\delta^{18}\text{O}$ Values in Atmospheric Nitrate

Modeling $\delta^{18}\text{O}$ values in atmospheric nitrate is more challenging relative to $\Delta^{17}\text{O}$ models for two reasons. First, unlike $\Delta\epsilon$ in the $\Delta^{17}\text{O}$ case, the KIE/equilibrium enrichment factors (ϵ) may be significant for the mass dependent reactions occurring during NO_x oxidation (i.e. R1–R6), but they are largely unknown. Second, the other oxygen sources (water, OH) that contribute to atmospheric nitrate have variable $\delta^{18}\text{O}$ values. This is unlike the $\Delta^{17}\text{O}$ modeling where all oxygen sources other than ozone are assumed to have a $\Delta^{17}\text{O}$ value ~ 0 . Variability of the $\delta^{18}\text{O}$ of water affects atmospheric nitrate isotopic composition both directly (R8) and indirectly (R6), adding complexity, because water $\delta^{18}\text{O}$ values vary significantly in time and space. Global 3D models simulating $\delta^{18}\text{O}$ of precipitation from first principles (i.e. Rayleigh distillations, temperature effects, equilibrium fractionations) are challenging tasks in and of themselves.

Recently, however, a relatively simple modeling approach has been used to predict $\delta^{18}\text{O}$ values in atmospheric nitrate (Mase 2010). Similar to the $\Delta^{17}\text{O}$ model, the isotope mass balance simplification was used and the unknown ϵ 's were ignored. However, the equilibrium enrichment factors between liquid water and vapor (30.18) and OH and water vapor (30.20) were taken into account. The atmospheric nitrate $\delta^{18}\text{O}$ mass balance equations, which are analogous to the $\Delta^{17}\text{O}$ mass balance, are given as:

$$\delta^{18}\text{ONO}_2 = \phi \delta^{18}\text{OO}_3 + (1 - \phi) \delta^{18}\text{OO}_2 \quad (30.27)$$

$$\delta^{18}\text{ONO}_3(\gamma) = \delta^{18}\text{ONO}_2(2/3) + 1/3 \delta^{18}\text{OOH} \quad (30.28)$$

$$\delta^{18}\text{OHNO}_3(\eta) = 2/3 \delta^{18}\text{ONO}_2 + 1/3 \delta^{18}\text{OO}_3 \quad (30.29)$$

$$\delta^{18}\text{O HNO}_3(\varphi) = 4/6 \delta^{18}\text{ONO}_2 + 1/6 \delta^{18}\text{OO}_3 + 1/6 \delta^{18}\text{OH}_2\text{O}_{\text{liq}} \quad (30.30)$$

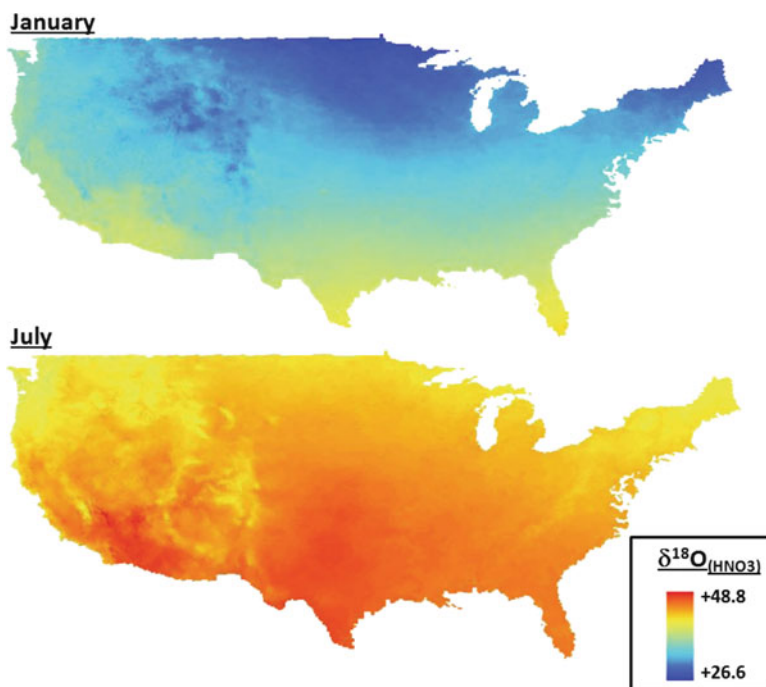
The $\delta^{18}\text{O}$ of liquid water was taken from interpolation of the GNIP data set (Fig. 30.5). The derivation of the $\delta^{18}\text{O}$ of O_3 and OH is discussed in Sects. 30.5.1 and 30.5.3 respectively. The temperature and pressure data was obtained from the NARR data set. For a given location, the daily average ϕ , γ , η , and φ are calculated using ISO-RACM.

As an example, Fig. 30.13 shows the $\delta^{18}\text{O}$ values of atmospheric nitrate for January and June, 2001. In these two cases, we fixed parameters ϕ , γ , η , and φ at values of 0.95, 0.65, 0.3, and 0.05 respectively. This shows that $\delta^{18}\text{O}$ variations are driven by factors other than simply the changes in NO_x oxidation pathways. These factors are spatial changes in $\delta^{18}\text{O}$ of the water and temperature that impact the $\delta^{18}\text{O}$ of the equilibrium water, and thus OH $\delta^{18}\text{O}$ (Figs. 30.8 and 30.9), and the $\delta^{18}\text{O}$ of ozone (Fig. 30.6). Clearly this isotope mass balance approach has some limitations, primarily through the use of daily average oxidation parameters (instead of an hourly time step), average temperatures, monthly resolution on the $\delta^{18}\text{O}$ of water and ignoring KIEs. The model predicts that atmospheric nitrate $\delta^{18}\text{O}$ values over North America would seasonally span $\sim 25\%$, with lower values occurring in the winter. This agrees with the seasonal trends for a given dataset in Fig. 30.2, but the absolute values are lower than observations by $\sim 10\text{--}20\%$. This is primarily due to the very negative $\delta^{18}\text{O}$ values assigned to OH that is based for $\text{H}_2\text{O}\text{--OH}$ equilibrium (Fig. 30.9). It is likely that the highly reactive OH is isotopically enriched by KIE during the oxidation of reduced compounds in the atmosphere.

In addition, exchange reactions between NO_x and OH (Zahn et al. 2006) may be important and increases OH's $\delta^{18}\text{O}$ and $\Delta^{17}\text{O}$ values over what would be expected based on water-OH equilibrium.

This approach to modeling atmospheric nitrate $\delta^{18}\text{O}$ values is crude, but it is also a first step. The model show that while the variations in atmospheric nitrate $\Delta^{17}\text{O}$ values are driven almost exclusively by shifts in chemical pathways, the $\delta^{18}\text{O}$ variability is likely a function of both chemistry, the $\delta^{18}\text{O}$ of local water in the atmosphere, and temperature. Why might

Fig. 30.13 Simulated $\delta^{18}\text{O}$ values of atmospheric nitrate for January and July 1, 2001 for the continental US. Values are calculated using methods described in the text



modeling $\delta^{18}\text{O}$ values in atmospheric nitrate be useful? If this can be done accurately it can be a way of estimating the $\delta^{18}\text{O}$ in atmospheric nitrate deposition over extended areas and timeframes. This data could be used as the atmospheric nitrate component in end member isotopic mixing models that try to use nitrate $\delta^{18}\text{O}$ values as a tracer of different N sources in watersheds (see Burns and Kendall 2002; Campbell et al. 2002). In addition, it might be a secondary constraint on oxidation chemistry that could be used in conjunction with the $\Delta^{17}\text{O}$ values. In particular, the incorporation of water, whose $\delta^{18}\text{O}$ values are highly variable in space and time, may be a way of tracing the importance of the N_2O_5 oxidation pathway.

30.7 Future Directions

There is a tremendous amount of science still needed for interpreting isotopic variation in atmospheric nitrate, but the potential outcomes will be well worth the effort. The first and foremost need is an expanded observational data set. Given the potential use of oxygen isotopes in the atmospheric nitrate system (understanding chemical pathways, the feedbacks between

climate and chemistry), the lack of data is surprising. This is largely due to limitations of the dual inlet methods that require relatively large amount of nitrate (Sect. 30.2). With new continuous flow techniques, this limitation has been lifted, which opens the way for wider spatial and better temporal measurements of both $\delta^{18}\text{O}$ and $\Delta^{17}\text{O}$ in atmospheric nitrate. Since the models predict strong $\Delta^{17}\text{O}$ variations under different chemical and meteorological conditions, the potential for verifying and improving the predictive capability of the models relies on observations from a wide range of environments. Data that compares urban vs. rural, high aerosol vs. low aerosol environments, different forested ecosystems where volatile organic emissions are high (deciduous, evergreen, tropical rainforest), latitudinal and longitudinal gradients, ocean vs. continental, and diurnal/hourly variability are just a few examples. Assessing isotope variation in the different phases (Elliott et al. 2009) of atmospheric nitrate ($\text{HNO}_{3(\text{g})}$, particulate nitrate and dissolved NO_3^-) and in different aerosol sizes would also be helpful for both understanding the fundamental chemical processes that form atmospheric nitrate and its isotopic variability.

Additional experiments investigating isotope effects in the NO_x -nitrate system are also needed.

Assessing the dependence of ozone's $\Delta^{17}\text{O}$ and $\delta^{18}\text{O}$ values on changes in temperature and pressure are primary in this regard. Direct determination of isotope effects in NO_x through experiments, instead of inferences using ozone data and reaction dynamics, would help to reduce uncertainties. Whether water contributes only one oxygen atom during N_2O_5 hydrolysis or if additional exchange occurs also needs to be addressed. An experimental investigation of the isotope effect of HO_2 formation and subsequent NO oxidation is important because current models assume any associated $\Delta^{17}\text{O}$ effect to be negligible. In order to interpret polar region data, the transfer coefficients and gas phase exchange reactions of oxidized halogens (BrO_x , ClO_x) need to be determined. There is almost no experimental data on some of the key mass dependent processes that might influence $\delta^{18}\text{O}$ and $\delta^{15}\text{N}$ in atmospheric nitrate. It is likely that the temperature sensitive $\text{NH}_4\text{NO}_3 \leftrightarrow \text{HNO}_3 + \text{NH}_3$ equilibrium will have a significant mass dependent effect, which should be determined experimentally.

A number of advances in the modeling approaches that try to simulate atmospheric nitrate oxygen isotope variations are also possible. Nitrate's short atmospheric lifetime and sensitivity to local scale trace gas concentrations would suggest that higher resolution 3D regional models would do a better job of simulating data. Adapting regional modeling platforms such as CMAQ or WRF-Chem to the atmospheric nitrate problem would be very beneficial. The models also must be kept up to date with new data from experimental work as discussed above. Incorporating equilibrium and KIE into model chemistry mechanisms for a more robust simulation of $\delta^{18}\text{O}$ and $\delta^{15}\text{N}$ variability would be an ambitious, long-term goal. This would require experimental and theoretical determination of a large number of KIE and photolysis effects that are quite challenging.

References

- Alexander B, Hastings MG, Allman DJ et al (2009) Quantifying atmospheric nitrate formation pathways based on a global model of the oxygen isotopic composition ($\Delta^{17}\text{O}$) of atmospheric nitrate. *Atmos Chem Phys* 9:5043–5056
- Amberger A, Schmidt HL (1987) Natural isotope content of nitrate as an indicator of its origin. *Geochim Cosmochim Acta* 51:2699–2705
- Araguas-Araguas L, Froehlich K, Rozanski K (2000) Deuterium and oxygen-18 isotope composition of precipitation and atmospheric moisture. *Hydrol Process* 14:1341–1355
- Barkan E, Luz B (2003) High-precision measurements of $^{17}\text{O}/^{16}\text{O}$ and $^{18}\text{O}/^{16}\text{O}$ of O_2 and O_2/Ar ratio in air. *Rapid Commun Mass Spectrom* 17:2809–2814
- Barkan E, Luz B (2005) High precision measurements of $^{17}\text{O}/^{16}\text{O}$ and $^{18}\text{O}/^{16}\text{O}$ ratios in H_2O . *Rapid Commun Mass Spectrom* 19:3737–3742
- Bhattacharya SK, Pandey A, Savarino J (2008) Determination of intramolecular isotope distribution of ozone by oxidation reaction with silver metal. *J Geophys Res* 113. doi:10.1029/2006JD008309
- Bobbink R, Hicks K, Galloway J et al (2010) Global assessment of nitrogen deposition effects on terrestrial plant diversity: a synthesis. *Ecol Appl* 20:30–59
- Böhlke JK, Mroczkowski SJ, Coplen TB (2003) Oxygen isotopes in nitrate: new reference materials for $^{18}\text{O}/^{17}\text{O}/^{16}\text{O}$ measurements and observations on nitrate-water equilibration. *Rapid Commun Mass Spectrom* 17:1835–1846
- Bowen GJ, Revenaugh J (2003) Interpolating the isotopic composition of modern meteoric precipitation. *Water Resour Res* 39. doi:10.1029/2003WR002086
- Brown SS, Stark H, Ryerson TB et al (2003) Nitrogen oxides in the nocturnal boundary layer: simultaneous in situ measurements of NO_3 , N_2O_5 , NO_2 , NO , and O_3 . *J Geophys Res* 108. doi:10.1029/2002JD002917
- Buda AR, DeWalle DR (2009) Using atmospheric chemistry and storm track information to explain the variation of nitrate stable isotopes in precipitation at a site in central Pennsylvania, USA. *Atmos Environ* 43:4453–4464
- Bunton CA, Halevi EA, Llewellyn DR (1952) Oxygen exchange between nitric acid and water. Part 1. *J Chem Soc*: 4913–4916
- Burns DA, Kendall C (2002) Analysis of $\delta^{15}\text{N}$ and $\delta^{18}\text{O}$ to differentiate NO_3^- sources at two watersheds in the Catskill Mountains of New York. *Water Resour Res* 38. doi:10.1029/2001WR000292
- Campbell DH, Kendall C, Chang CCY et al (2002) Pathways for nitrate release from an alpine watershed: determination using $\delta^{15}\text{N}$ and $\delta^{18}\text{O}$. *Water Resour Res* 38. doi:10.1029/2001WR000294
- Casciotti KL, Sigman DM, Hastings MG et al (2002) Measurement of the oxygen isotopic composition of nitrate in seawater and freshwater using the denitrifier method. *Anal Chem* 74:4905–4912
- Chang CCY, Langston J, Riggs M et al (1999) A method for nitrate collection for $\delta^{15}\text{N}$ and $\delta^{18}\text{O}$ analysis from waters with low nitrate concentrations. *Can J Fish Aquat Sci* 56:1856–1864
- Cliff SS, Thiemens MH (1994) High precision isotopic determination of the $^{18}\text{O}/^{16}\text{O}$ and $^{17}\text{O}/^{16}\text{O}$ ratio in nitrous oxide. *Anal Chem* 66:2791–2793
- Dieke GH, Crosswhite HM (2010) The ultraviolet bands of OH fundamental data. *J Quant Spectrosc Radiat Transfer* 111: 1516–1542
- Dole M, Lane GA, Rudd DP et al (1954) Isotopic composition of atmospheric oxygen and nitrogen. *Geochim Cosmochim Acta* 6:65–78
- Dubey MK, Mohrshchladt R, Donahue NM, Anderson JG (1997) Isotope-specific kinetics of hydroxyl radical (OH) with water

- (H₂O): testing models of reactivity and atmospheric fractionation. *J Phys Chem A* 101:1494–1500
- Durka W, Schulze ED, Gebauer G et al (1994) Effects of forest decline on uptake and leaching of deposited nitrate determined from ¹⁵N and ¹⁸O measurements. *Nature* 372: 765–767
- Elliott EM, Kendall C, Boyer EW et al (2009) Dual nitrate isotopes in dry deposition: utility for partitioning NO_x source contributions to landscape nitrogen deposition. *J Geophys Res* 114. doi:[10.1029/2008JG000889](https://doi.org/10.1029/2008JG000889)
- Freyer HD (1991) Seasonal-variation of ¹⁵N/¹⁴N ratios in atmospheric nitrate species. *Tellus Ser B* 43:30–44
- Galloway JN (1995) Acid deposition: perspectives in time and space. *Water Air Soil Pollut* 85:15–24
- Galloway JN (1998) The global nitrogen cycle: changes and consequences. *Environ Pollut* 102:15–24
- Galloway JN, Dentener FJ, Capone DG et al (2004) Nitrogen cycles: past, present, and future. *Biogeochemistry* 70: 153–226
- Gao YQ, Marcus RA (2001) Strange and unconventional isotope effects in ozone formation. *Science* 293:259–263
- Gat JR (1996) Oxygen and hydrogen isotopes in the hydrologic cycle. *Annu Rev Earth Planet Sci* 24:225–262
- Gellene GI (1996) An explanation for symmetry-induced isotopic fractionation in ozone. *Science* 274:1344–1346
- Guenther J, Krankowsky D, Mauersberger K (2000) Third-body dependence of rate coefficients for ozone formation in ¹⁶O/¹⁸O mixtures. *Chem Phys Lett* 324:31–36
- Hales HC, Ross DS, Lini A (2007) Isotopic signature of nitrate in two contrasting watersheds of Brush Brook, Vermont, USA. *Biogeochemistry* 84:51–66
- Hallquist M, Stewart DJ, Baker J et al (2000) Hydrolysis of N₂O₅ on submicron sulfuric acid aerosols. *J Phys Chem A* 104:3984–3990
- Hastings MG, Sigman DM, Lipschultz F (2003) Isotopic evidence for source changes of nitrate in rain at Bermuda. *J Geophys Res* 108. doi:[10.1029/2003JD003789](https://doi.org/10.1029/2003JD003789)
- Hathorn BC, Marcus RA (1999) An intramolecular theory of the mass-independent isotope effect for ozone. I. *J Chem Phys* 111:4087–4100
- Hathorn BC, Marcus RA (2000) An intramolecular theory of the mass-independent isotope effect for ozone II. Numerical implementation at low pressures using a loose transition state. *J Chem Phys* 113:9497–9509
- Heidenreich JE III, Thiemens MH (1983) A non-mass-dependent isotope effect in the production of ozone from molecular oxygen. *J Chem Phys* 78:892–895
- Herzberg G (1966) Infrared and Raman spectra of polyatomic molecules, 2nd edn. Krieger, Malabar
- Horita J, Wesolowski DJ (1994) Liquid-vapor fractionation of oxygen and hydrogen isotopes of water from the freezing to the critical-temperature. *Geochim Cosmochim Acta* 58: 3425–3437
- Jaegle L, Jacob DJ, Brune WH et al (2000) Photochemistry of HO_x in the upper troposphere at northern midlatitudes. *J Geophys Res* 105:3877–3892
- Johnston JC, Thiemens MH (1997) The isotopic composition of tropospheric ozone in three environments. *J Geophys Res* 102:25395–25404
- Kaiser J (2009) Reformulated ¹⁷O correction of mass spectrometric stable isotope measurements in carbon dioxide and a critical appraisal of historic absolute carbon and oxygen isotope ratios. *Geochim Cosmochim Acta* 72:1312–1334
- Kaiser J, Hastings MG, Houlton BZ et al (2007) Triple oxygen isotope analysis of nitrate using the denitrifier method and thermal decomposition of N₂O. *Anal Chem* 79:599–607
- Kalnay E, Kanamitsu M, Kistler R et al (1996) The NCEP/NCAR 40-year reanalysis project. *Bull Am Meteorol Soc* 77:437–471
- Kendall C (1998) Tracing nitrogen sources and cycling in catchments. Elsevier Science B.V, Amsterdam, pp 519–576
- Komatsu DD, Ishimura T, Nakagawa F et al (2008) Determination of the ¹⁵N/¹⁴N, ¹⁷O/¹⁶O, and ¹⁸O/¹⁶O ratios of nitrous oxide by using continuous-flow isotope-ratio mass spectrometry. *Rapid Commun Mass Spectrom* 22:1587–1596
- Kornel BE, Gehre M, Hoffling R et al (1999) On-line δ¹⁸O measurement of organic and inorganic substances. *Rapid Commun Mass Spectrom* 13:1685–1693
- Krankowsky D, Bartecki F, Klees GG et al (1995) Measurement of heavy isotope enrichment in tropospheric ozone. *Geophys Res Lett* 22:1713–1716
- Krankowsky D, Lammerzahl P, Mauersberger K (2000) Isotopic measurements of stratospheric ozone. *Geophys Res Lett* 27:2593–2595
- Kunasek SA, Alexander B, Steig EJ et al (2008) Measurements and modeling of Δ¹⁷O of nitrate in snowpits from Summit, Greenland. *J Geophys Res* 113. doi:[10.1029/2008JD010103](https://doi.org/10.1029/2008JD010103)
- Liang MC, Irion FW, Weibel JD et al (2006) Isotopic composition of stratospheric ozone. *J Geophys Res* 111. doi:[10.1029/2005JD006342](https://doi.org/10.1029/2005JD006342)
- Luz B, Barkan E (2005) The isotopic ratios ¹⁷O/¹⁶O and ¹⁸O/¹⁶O in molecular oxygen and their significance in biogeochemistry. *Geochim Cosmochim Acta* 69:1099–1110
- Lyons JR (2001) Transfer of mass-independent fractionation in ozone to other oxygen-containing radicals in the atmosphere. *Geophys Res Lett* 28:3231–3234
- Majoube M (1971) Oxygen-18 and deuterium fractionation between water and steam. *J Chim Phys Physicochim Biol* 68:1423–1436
- Martin RV, Sauvage B, Folkens I et al (2007) Space-based constraints on the production of nitric oxide by lightning. *J Geophys Res* 112. doi:[10.1029/2006JD007831](https://doi.org/10.1029/2006JD007831)
- Mase D (2010) A coupled modeling and observational approach to understanding the ¹⁵N and ¹⁸O of atmospheric nitrate. M.S. Thesis, Purdue University
- Matsuhisa Y, Goldsmith JR, Clayton RN (1978) Mechanisms of hydrothermal crystallization of quartz at 250°C and 15 kbar. *Geochim Cosmochim Acta* 42:173–182
- Mauersberger K, Lammerzahl P, Krankowsky D (2001) Stratospheric ozone isotope enrichments-revisited. *Geophys Res Lett* 28:3155–3158
- Mauersberger K, Krankowsky D, Janssen C (2003) Oxygen isotope processes and transfer reactions. *Space Sci Rev* 106:265–279
- McCabe JR, Thiemens MH, Savarino J (2007) A record of ozone variability in South Pole Antarctic snow: role of

- nitrate oxygen isotopes. *J Geophys Res* 112. doi:[10.1029/2006JD007822](https://doi.org/10.1029/2006JD007822)
- McIlvin MR, Altabet MA (2005) Chemical conversion of nitrate and nitrite to nitrous oxide for nitrogen and oxygen isotopic analysis in freshwater and seawater. *Anal Chem* 77: 5589–5595
- Meijer HAJ, Li WJ (1998) The use of electrolysis for accurate $\delta^{17}\text{O}$ and $\delta^{18}\text{O}$ isotope measurements in water. *Isotopes Environ Health Stud* 34:349–369
- Mentel TF, Sohn M, Wahner A (1999) Nitrate effect in the heterogeneous hydrolysis of dinitrogen pentoxide on aqueous aerosols. *Phys Chem Chem Phys* 1:5451–5457
- Michalski G (2009) Purification procedure for $\delta^{15}\text{N}$, $\delta^{18}\text{O}$, $\Delta^{17}\text{O}$ analysis of nitrate. *Int J Environ Anal Chem* 90:586–590
- Michalski G, Bhattacharya SK (2009) The role of symmetry in the mass independent isotope effect in ozone. *Proc Natl Acad Sci U S A* 106:11496–11501
- Michalski G, Xu F (2010) Isotope modeling of nitric acid formation in the atmosphere using ISO-RACM: testing the importance of nitric oxide oxidation, heterogeneous reactions, and trace gas chemistry. *Atmos Chem Phys* (in review)
- Michalski G, Savarino J, Böhlke JK et al (2002) Determination of the total oxygen isotopic composition of nitrate and the calibration of a $\Delta^{17}\text{O}$ nitrate reference material. *Anal Chem* 74:4989–4993
- Michalski G, Scott Z, Kabling M et al (2003) First measurements and modeling of $\Delta^{17}\text{O}$ in atmospheric nitrate. *Geophys Res Lett* 30:1870. doi:[10.1029/2003GL017015](https://doi.org/10.1029/2003GL017015)
- Michalski G, Bhattacharya SK, Girsch G (In preparation) Isotope effects occurring during the NO_x cycle
- Miller MF (2002) Isotopic fractionation and the quantification of ^{17}O anomalies in the oxygen three-isotope system: an appraisal and geochemical significance. *Geochim Cosmochim Acta* 66:1881–1889
- Morin S, Savarino J, Bekki S et al (2007) Signature of Arctic surface ozone depletion events in the isotope anomaly ($\Delta^{17}\text{O}$) of atmospheric nitrate. *Atmos Chem Phys* 7: 1451–1469
- Morin S, Savarino J, Frey MM et al (2008) Tracing the origin and fate of NO_x in the Arctic atmosphere using stable isotopes in nitrate. *Science* 322:730–732
- Morin S, Savarino J, Frey MM et al (2009) Comprehensive isotopic composition of atmospheric nitrate in the Atlantic Ocean boundary layer from 65°S to 79°N . *J Geophys Res* 114. doi:[10.1029/2008JD010696](https://doi.org/10.1029/2008JD010696)
- Morton J, Barnes J, Schueler B et al (1990) Laboratory studies of heavy ozone. *J Geophys Res* 95:901–907
- Mosier A, Kroeze C, Nevison C et al (1998) Closing the global N_2O budget: nitrous oxide emissions through the agricultural nitrogen cycle. *Nutr Cycl Agroecosyst* 52:225–248
- Patris N, Cliff SS, Quinn PK et al (2007) Isotopic analysis of aerosol sulfate and nitrate during ITCT-2k2: determination of different formation pathways as a function of particle size. *J Geophys Res* 112:D23301. doi:[10.1029/2005JD006214](https://doi.org/10.1029/2005JD006214)
- Peiro-Garcia J, Nebot-Gil I (2002) Ab initio study of the mechanism and thermochemistry of the atmospheric reaction $\text{NO} + \text{O}_3 \rightarrow \text{NO}_2 + \text{O}_2$. *J Phys Chem A* 106:10302–10310
- Revesz K, Böhlke JK (2002) Comparison of $\delta^{18}\text{O}$ in nitrate by different combustion techniques. *Anal Chem* 74: 5410–5413
- Revesz K, Böhlke JK, Yoshinari T (1997) Determination of $\delta^{18}\text{O}$ and $\delta^{15}\text{N}$ in nitrate. *Anal Chem* 69:4375–4380
- Rodhe H, Dentener F, Schulz M (2002) The global distribution of acidifying wet deposition. *Environ Sci Technol* 36: 4382–4388
- Savarino J, Lee CCW, Thiemens MH (2000) Laboratory oxygen isotopic study of sulfur (IV) oxidation: origin of the mass-independent oxygen isotopic anomaly in atmospheric sulfates and sulfate mineral deposits on Earth. *J Geophys Res* 105:29079–29088
- Savarino J, Kaiser J, Morin S et al (2007) Nitrogen and oxygen isotopic constraints on the origin of atmospheric nitrate in coastal Antarctica. *Atmos Chem Phys* 7:1925–1945
- Savarino J, Bhattacharya SK, Morin S et al (2008) The $\text{NO} + \text{O}_3$ reaction: a triple oxygen isotope perspective on the reaction dynamics and atmospheric implications for the transfer of the ozone isotope anomaly. *J Chem Phys* 128. doi:[10.1063/1.2917581](https://doi.org/10.1063/1.2917581)
- Silva SR, Kendall C, Wilkison DH et al (2000) A new method for collection of nitrate from fresh water and the analysis of nitrogen and oxygen isotope ratios. *J Hydrol* 228:22–36
- Spoelstra J, Schiff SL, Elgood RJ et al (2001) Tracing the sources of exported nitrate in the Turkey Lakes Watershed using $^{15}\text{N}/^{14}\text{N}$ and $^{18}\text{O}/^{16}\text{O}$ isotopic ratios. *Ecosystems* 4: 536–544
- Stockwell WR, Kirchner F, Kuhn M et al (1997) A new mechanism for regional atmospheric chemistry modeling. *J Geophys Res* 102:25847–25879
- Thiemens MH, Heidenreich JE III (1983) The mass-independent fractionation of oxygen: a novel isotope effect and its possible cosmochemical implications. *Science* 219:1073–1075
- Thiemens MH, Jackson T (1990) Pressure dependency for heavy isotope enhancement in ozone formation. *Geophys Res Lett* 17:717–719
- Thiemens MH, Jackson T, Mauersberger K, Schueler B, Morton J (1991) Oxygen isotope fractionation in stratospheric CO_2 . *Geophys Res Lett* 18:669–672
- Thiemens MH, Savarino J, Farquhar J et al (2001) Mass-independent isotopic compositions in terrestrial and extraterrestrial solids and their applications. *Acc Chem Res* 34: 645–652
- Tuazon EC, Atkinson R, Plum CN et al (1983) The reaction of gas-phase N_2O_5 with water-vapor. *Geophys Res Lett* 10: 953–956
- Uemura R, Barkan E, Abe O et al (2010) Triple isotope composition of oxygen in atmospheric water vapor. *Geophys Res Lett* 37. doi:[10.1029/2009GL041960](https://doi.org/10.1029/2009GL041960)
- Urey HC (1947) Thermodynamic properties of isotopic substances. *J Chem Soc*:562–581
- Valentini JJ (1987) Mass-independent isotopic fractionation in nonadiabatic molecular-collisions. *J Chem Phys* 86: 6757–6765
- Vuille M, Werner M, Bradley RS et al (2005) Stable isotopes in precipitation in the Asian monsoon region. *J Geophys Res* 110:D23108. doi:[10.1029/2005JD006022](https://doi.org/10.1029/2005JD006022)
- Wahner A, Mentel TF, Sohn M (1998) Gas-phase reaction of N_2O_5 with water vapor: importance of heterogeneous hydrolysis of N_2O_5 and surface desorption of HNO_3 in a large teflon chamber. *Geophys Res Lett* 25:2169–2172

- Wassenaar LI (1995) Evaluation of the origin and fate of nitrate in the Abbotsford Aquifer using the isotopes of ^{15}N and ^{18}O in NO_3^- . *Appl Geochem* 10:391–405
- Wild O, Law KS, McKenna DS et al (1996) Photochemical trajectory modeling studies of the North Atlantic region during August 1993. *J Geophys Res* 101:29269–29288
- Williard KWJ, DeWalle DR, Edwards PJ, Sharpe WE (2001) ^{18}O isotopic separation of stream nitrate sources in mid-Appalachian forested watersheds. *J Hydrol* 252:174–188
- Yung YL, DeMore WB, Pinto JP (1991) Isotopic exchange between carbon dioxide and ozone via $\text{O}(^1\text{D})$ in the stratosphere. *Geophys Res Lett* 18:13–16
- Yvon SA, Plane JMC, Nien CF et al (1996) Interaction between nitrogen and sulfur cycles in the polluted marine boundary layer. *J Geophys Res* 101:1379–1386
- Zahn A, Franz P, Bechtel C, Grooß JU, Röckmann T (2006) Modelling the budget of middle atmospheric water vapour isotopes. *Atmos Chem Phys* 6:2073–2090
- Zhang Y, Seigneur C, Seinfeld JH et al (2000) A comparative review of inorganic aerosol thermodynamic equilibrium modules: similarities, differences, and their likely causes. *Atmos Environ* 34:117–137